ISSN: 2249-8958

International Journal of Engineering & Advanced Technology (IJEAT)

Volume No. 12
Issue No. 3
September - December 2024

ENRICHED PUBLICATIONS PVT. LTD

JE-18, Gupta Colony, Khirki, Extn, Malviya Nagar, New Delhi-110017
PHONE : - + 91-8877340707
E-Mail : info@enrichedpublications.com

ISSN: 2249-8958

International Journal of Engineering & Advanced Technology (IJEAT)

Aim & Scope

AIM

International Journal of Engineering & Advanced Technology (IJEAT) is having ISSN 2249-8958 (online), bi-monthly (Online) and Tri-Annually (Print) international journal, being published in the months of February, April, June, August, October and December by Blue Eyes Intelligence Engineering & Sciences Publication (BEIESP) Bhopal (M.P.), India since year 2011 and processed papers will be forwarded for inclusion in the SCOPUS database. It is academic, online, open access, peer reviewed international journal. The aim of the journal is to:

- •disseminate original, scientific, theoretical or applied research in the field of Engineering and allied fields.
- •dispense a platform for publishing results and research with a strong empirical component.
- •aqueduct the significant gap between research and practice by promoting the publication of original, novel, industry-relevant research.
- •seek original and unpublished research papers based on theoretical or experimental works for the publication globally.
- •publish original, theoretical and practical advances in Computer Science & Engineering, Information Technology, Electrical and Electronics Engineering, Electronics and Telecommunication, Mechanical Engineering, Civil Engineering, Textile Engineering and all interdisciplinary streams of Engineering Sciences.
- •impart a platform for publishing results and research with a strong empirical component.
- •create a bridge for significant gap between research and practice by promoting the publication of original, novel, industry-relevant research.
- •solicit original and unpublished research papers, based on theoretical or experimental works.

SCOPE

International Journal of Engineering and Advanced Technology (IJEAT) covers all topics of all engineering branches. Some of them are Computer Science & Engineering, Information Technology, Electronics & Communication, Electrical and Electronics, Electronics and Telecommunication, Civil Engineering, Mechanical Engineering, Textile Engineering and all interdisciplinary streams of Engineering Sciences. The main topic includes but not limited to:

ISSN: 2249-8958

1.Smart Computing and Information Processing

2.Recent Trends in Microelectronics and VLSI Design

3.Challenges of Industry and their Solutions, Communications

4.Internet of Things (IoT)

5.Microwaves and Photonics

6.Computation Intelligence and Analytics

7.Energy Harvesting and Wireless Power Transmission

8.Advance Concept of Networking and Database

9.Machine Learning (ML) and Knowledge Mining (KM)

10.Advanced Computer networking Computational Intelligence

11.Communications

12.Algorithms and Complexity

13.Software Engineering and Knowledge Engineering

14.Computer Networks and Inventive Communication Technologies

15.Resent Engineering and Nano Technology

16.Recent on Mechanical Engineering and Technology

17.Advance Civil Engineering and Technology

ISSN: 2249-8958

Editor-in-Chief

Publication and Distribution Head

Members of Associate Editor-In-Chief Chair

Scientific Editors

ISSN: 2249-8958

Executive Editor Chair

Members of Executive Editor Chair

ISSN: 2249-8958

International Journal of Engineering & Advanced Technology (IJEAT)

(Volume No. 12, Issue No. 3, September - December 2024)

Contents

ISSN: 2249-8958

Performance Analysis of 6T, 8T and 10T SRAM Cell in 45nm Technology

M G Srinivasa, Bhavana M S

A B S T R A C T

The rise of portable battery-powered devices has emphasized the significance of low power IC design. Embedded SRAM units have become indispensable elements within contemporary SOCs due to their substantial footprint. In research circles, SRAM is highly regarded as a semiconductor memory type, highlighting its crucial role in the VLSI sector. In this paper, 6T, 8T and 10T SRAM cells design is estimated for power consumption and delay. This proposed work presents the schematic, simulation of analysis of 6T, 8T and 10T SRAM cells at 45 nm technology. The Cadence Virtuoso software is utilized for creating schematic diagrams and layouts, while the ASSURA library is employed for conducting design rule checks (DRC) and layout versus schematic (LVS) comparisons to verify the alignment between the layout and the schematic. In the process, a low VDD of 1 V is taken for the design. The results shows that 10T SRAM is efficient in terms of read and write delay and power consumptions.

Keywords: SRAM, Cadence. Tool, ASSURA, DRC, LVS

I. INTRODUCTION

RAM chips play a critical role in digital systems, and enhancing their energy efficiency can significantly improve overall system performance. SRAM cells, a common choice in RAM design, offer faster speeds and lower power usage compared to DRAM, making them preferred. With the growing demand for portable devices, minimizing power usage is a key concern in VLSI design. This has spurred interest in developing low-voltage nano-sized SRAMs. However, reducing their size has also increased MOSFET leakage current, leading to higher power consumption.

Consequently, there is increased emphasis on designing high-performance SRAMs, crucial for handheld devices, high-performance equipment, and processors. Voltage scaling is essential for achieving energy-efficient operation in digital circuits, reducing dynamic energy usage.

II. CIRCUIT DESIGN AND ANALYSIS

A. 6T SRAM Cell

An SRAM cell typically comprises six MOSFETs. Within an SRAM cell, each bit is stored using four transistors (P1, P2, N1 and N3) arranged in two cross-coupled inverters. Two additional access transistors (N2 and N4) regulate cell access during read and write operations. The activation of the word line WL governs the behavior of N2 and N4, determining whether the cell connects to the bit lines BL and BL` for data transfer during both reading and writing processes.

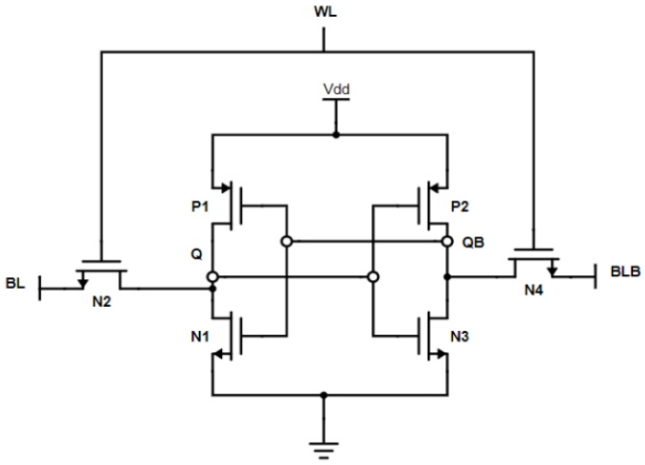

Fig.1: 6T SRAM Cell [6]

The SRAM cell has three states
1. Write
2. Read
3. Standby (Idle)

SRAM in read and write modes should exhibit "readability" and "write stability" separately.

The process of writing data starts with applying the intended value onto the bit lines. When writing a `0`, the bit lines are set to `0`, with BL` becoming `1` and BL becoming `0`, considering that the bit lines are initially charged to a high voltage. Conversely, to write a `1`, the states of BL and BL` are interchanged. After this, the word line (WL) is activated, facilitating the storage of the data into the cell [4].

During the reading process, the activation of the word line WL triggers the examination of the SRAM cell's state, accomplished through the involvement of a single access transistor (N4) and the bit line (BL). Owing to their extended length, bit line exhibits parasitic capacitance. The reading procedure commences by pre-charging both bit lines to VDD.

The extraction of output occurs from these bit lines throughout the reading operation. In contrast, when data is being written into the memory cell, the application of values onto the bit lines occurs simultaneously with the activation of the word line WL, which consequently activates both access transistors (N2 and N4) linked to the bit lines. This activation leads to a reduction in BL's voltage [4,6].

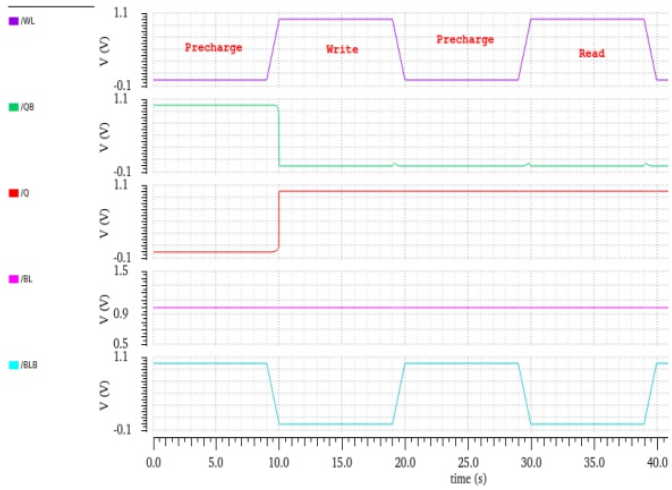

Fig 2: 6T SRAM Read and Write Operation

During the idle state, the word line is set to a low state, deactivating the access transistors. This action disconnects the inverters connected in a cross-coupled configuration from the bit lines via N2 and N4. As long as they remain connected to VDD. The two cross-coupled inverters formed by P1-N1 and P2-N3 will sustain each other, preserving the stored value in the SRAM.B.

8T SRAM Cell

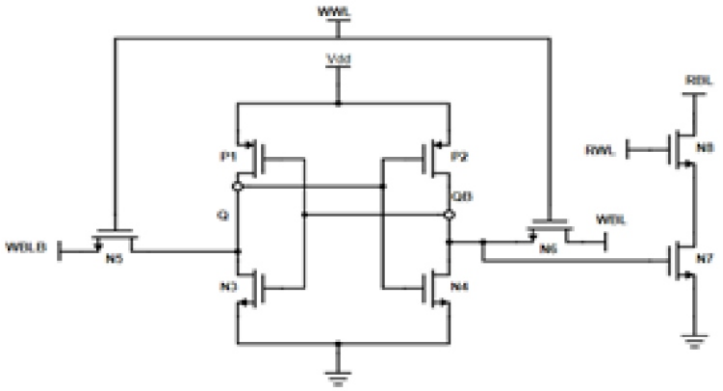

Fig 3: 8T SRAM Cell [7]

The 8T SRAM cell features distinct pathways for read and write operations, ensuring robust stability for both processes and serving as an effective design approach for SRAM cells. It comprises two-bit lines (WBL and WBLB) linked via NMOS access transistors N5 and N6 to the cross-coupled inverters. Additionally, the wire storing the bit connects to the gate of transistor N7, with its source linked to VSS [9][13][14].

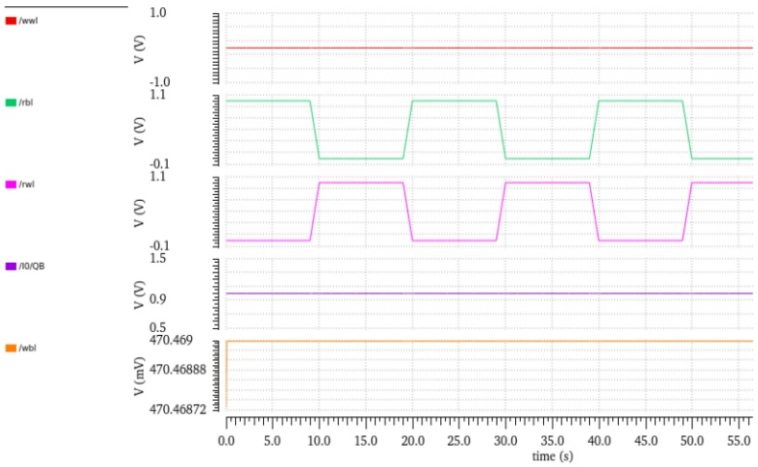

Fig 4: 8T SRAM Read Operation

The drain of transistor N7 is linked to the source of transistor N8, and the Read Word Line (RWL) controls the read operation by acting on the gate of N8. The Read Bit Line (RBL) is initially pre-charged to VDD and serves as the output during reading. When RWL is activated, transistor N5 turns on, and with the subsequent activation of N6 through RWL, the stored charge is drained, providing acomplementary output for writing bit 1 through BL. This configuration utilizes pass transistors in the read pathway, with RWL controlling them through their connection to the gate of these pass transistors.

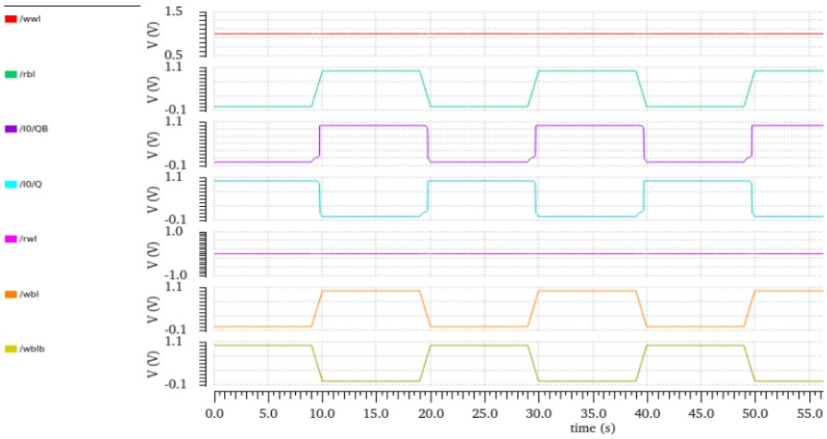

Fig 5: 8T SRAM write Operation

During write operation RWL is made low and complementary inputs are applied to WBL and WBLB. Outputs are observed in Q and QB nodes [2].

C. 10T SRAM Cell

The 10T SRAM consists of two cross coupled transistors P1, N3 and P2, N4 with two access transistors N5, N6. A separate read port of four transistors P3, N10, N8 and N9. The presence of extra transistors serves to interrupt the leakage current path from RBL when RWL is low, ensuring its independence from the current of data storage nodes [1][10][11][12]. The write access mechanism and fundamental data storage unit resemble that of a standard 6T SRAM cell. The power consumed is less than the 10T SRAM that uses differential pair [8]

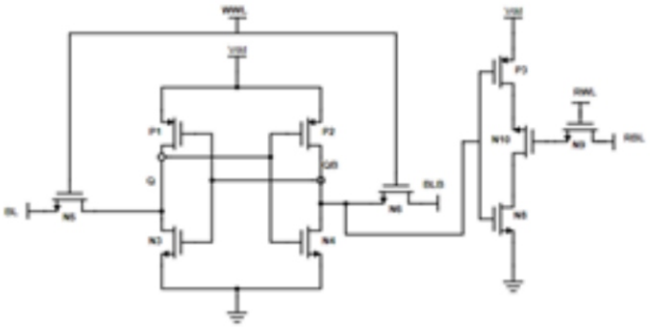

Fig 6: 10T SRAM Cell

Table.1: Power, Area, and Delay Analysis of SRAM Cells

SRAM	Read Power in µW	Write Power in µW	Read Delay in ms	Write Delay in ms	Power in W	Area in µm²
6T	1.5589	69.533	350.755	313.385	75.149n	4.158
8T	10.548	23.15	285.126	81.72	1.0939µ	9.801
10T	18.803	18.24	255.453	57.94	38.217n	10.045

During a write operation, the word line (WWL) and bit line (BL/BLB) are activated based on the address of the cell to be written. RWL is made low. The data to be written is placed on the BL and its complement (BLB). The access transistors (N5 and N6) are turned on by the activated WWL, allowing the data on BL/BLB to be written into the storage nodes of the SRAM cell [5].

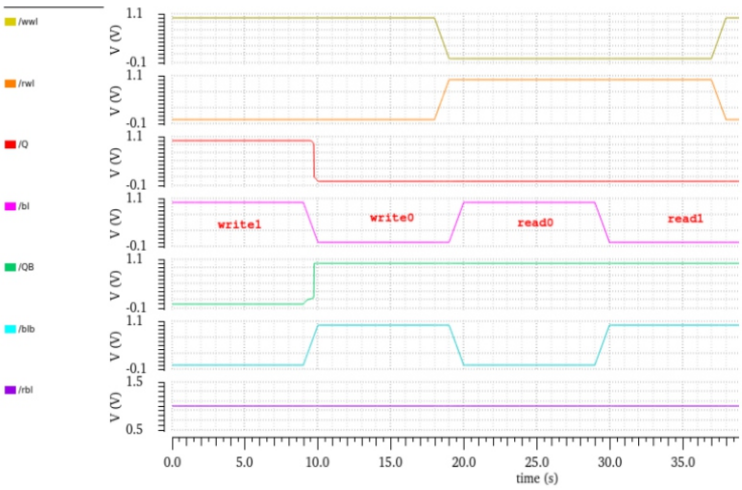

Fig 7: 10T SRAM Read and Write Operation

During a read operation, the word line (WWL) and RWL is made high. The access transistors connect the storage nodes to the bit lines (BL/BLB). The voltage levels on BL and BLB are sensed to determine the data stored in the SRAM cell. If BL is at a higher voltage level compared to BLB, it indicates a logic '1' stored in the cell and if BL is at a lower voltage level compared to BLB, it indicates a logic '0'.

III. RESULTS AND DISCUSSION

In conventional 6T SRAM Cell, N1 and P2 transistors have W/L ratio of 0.125 while all the other transistors have the ratio of 0.375. This is done to analyze the precharge, read and write stages clearly in the output. In 8T and 10T SRAM Cell, all the transistors have W/L ratio of 0.375. The supply voltage is 1V for the circuit.

The Table.1 (Column 2 and 3) and Fig. demonstrates the contrast between the power consumption for reading and writing of 6T, 8T and 10T SRAM Cells.

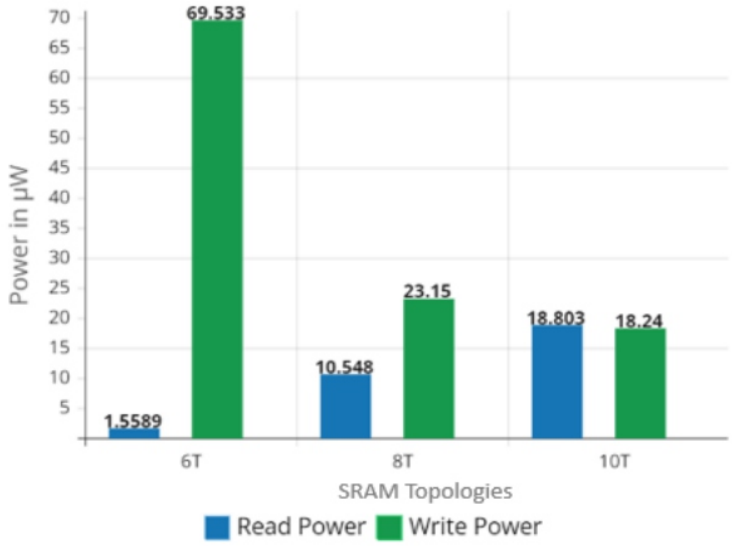

Fig 8: Comparison of Read and Write Power

Read power of 6T SRAM cell is 85.22% less than 8T. Read power of 6T SRAM cell is 91.7% less than 10T SRAM. Similarly, write power of 8T SRAM is 66.7% less than 6T SRAM. 10T SRAM has 73.76% of decreased write power than 6T SRAM. From this we observe that when read power increases at the same time write power decreases, with increase in transistor sizing [3].

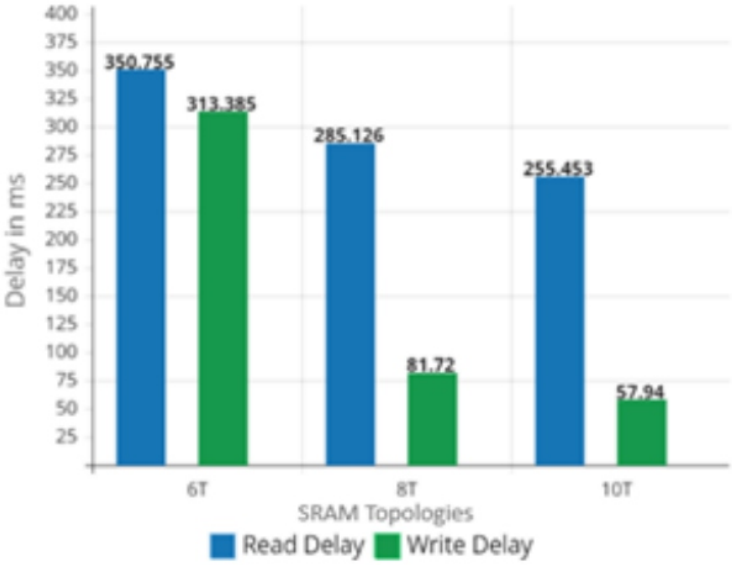

Fig 9: Comparison of Read and Write Delay

The Table.1 (Column 4 and 5) and Fig 9 shows the contrast between read and write delay of 6T, 8T and 10T SRAM Cells.

6T SRAM has a read delay 23.02% more than 8T SRAM and 37.31% more than 10T SRAM. Similarly, the write delay of 8T SRAM is 73.92% less than 6T SRAM and 10T SRAM has 81.51% less write delay than 6T SRAM. We observe that the read and write delay decreases as transistor sizing increases which indicates the increase in speed of SRAM cells with sizing.

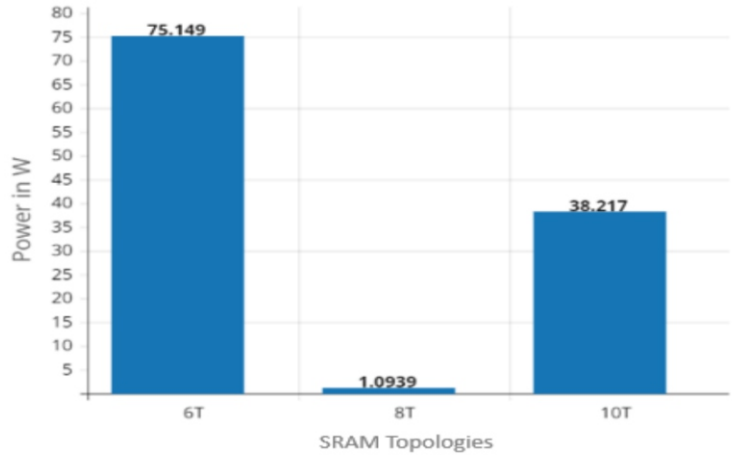

Fig 10: Comparison of Average Power

The Table.1 (Column 5 and 6) and Fig.10 illustrates the contrast between average power of 6T, 8T and 10T SRAM Cells. The average power of 10T is 45.01% less than 6T SRAM. It is also observed that it is less than average power of 8T SRAM. This indicates that 10T SRAM has less leakage power and is operating more efficiently when compared to other two SRAM cells. Fig. 11, 12, 13 shows the layout of

the SRAM cells.

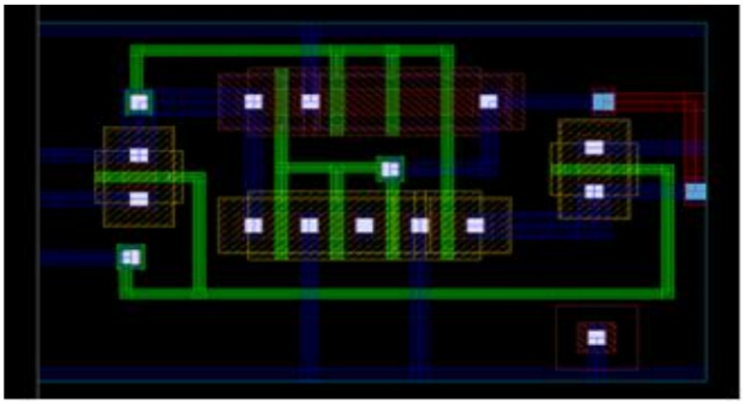

Fig 11: 6T SRAM Cell layout

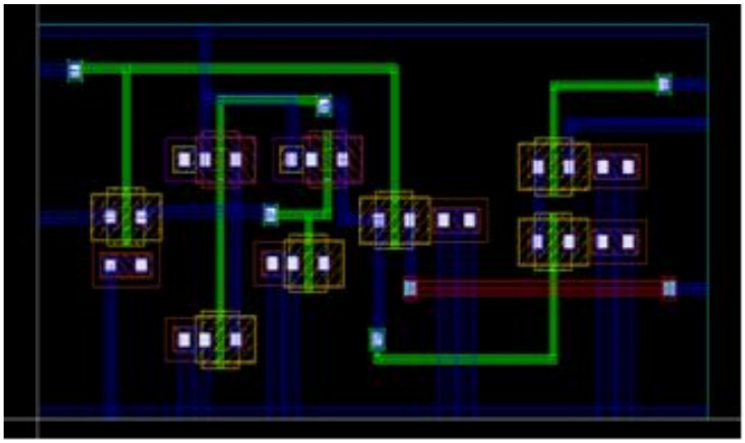

Fig 12: 8T SRAM Cell layout

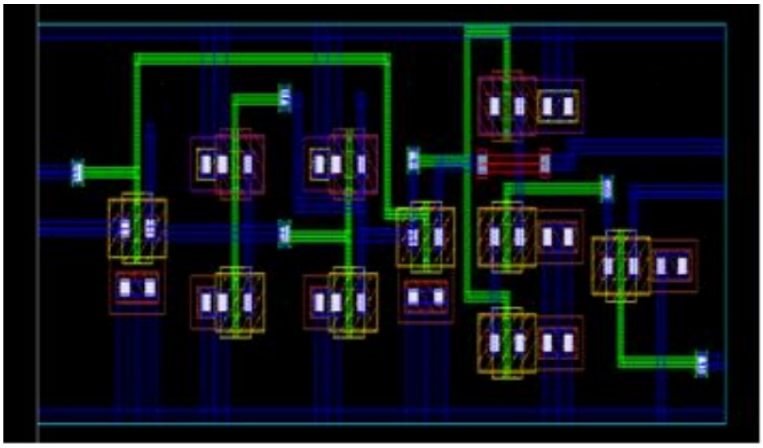

Fig.13: 10T SRAM Cell layout

IV. CONCLUSION

In this work standard 6T SRAM is compared with 8T and 10T SRAM cells in terms of read power, write power, read delay, write delay, and average power. 10T SRAM has thesame range of read and write power. 6T SRAM has more write power and more delay compared to other SRAM. 6T isefficient in terms of read power but if we consider other parameters 10T SRAM cell is found to be more efficient compared to 6T and 8T.

DECLARATION STATEMENT

Funding	No, I did not receive.
Conflicts of Interest	No conflicts of interest to the best of our knowledge.
Ethical Approval and Consent to Participate	No, the article does not require ethical approval and consent to participate with evidence.
Availability of Data and Material	Not relevant.
Authors Contributions	All authors have equal participation in this article.

REFERENCES

1. Rukkumani. V, Devarajan N, "Design and Analysis of static random-access memory by Schmitt trigger topology for low voltage application," in Journal of Engineering Science and Technology, Vol. 11, No. 12 (2016) 1722 - 1735.

2. Tomar. V K, Vinay Kumar, "A Comparative Performance Analysis of 6T, 7T and 8T SRAM Cells in 18nm FinFET Technology," in International Conference on Power Electronics and IoT Applications in Renewable Energy and its Control (PARC), Mathura, India, 2020, pp. 329-333.

3. D. Mittal and V. K. Tomar, "Performance Evaluation of 6T, 7T, 8T, and 9T SRAM cell Topologies at 90 nm Technology Node," in 2020 11th International Conference on Computing, Communication and Networking Technologies (ICCCNT), Kharagpur, India, 2020, pp. 1-4. https://doi.org/10.1109/ICCCNT49239.2020.9225554

4. Pinki Narah, Sharmila Nath, "A Comparative Analysis of SRAM Cells in 45nm, 65nm, 90nm Technology," in Int. Journal of Engineering Research and Application, Vol. 8, Issue5 (Part -I), May 2018, pp31-36.

5. P. S. Grace and N. M. Sivamangai, "Design of 10T SRAM cell for high SNM and low power," in 2016 3rd International Conference on Devices, Circuits and Systems (ICDCS), Coimbatore, India, 2016, pp. 281-285. https://doi.org/10.1109/ICDCSyst.2016.7570609

6. R. Kumar et al., "Design and Benchmark of Iso-Stable High Density 4T SRAM cells for 64MB arrays in 65nm LSTP," in 2020 IEEE 17th India Council International Conference (INDICON), New Delhi, India, 2020, pp. 1-7.https://doi.org/10.1109/INDICON49873.2020.9342091

7. T Santhosh Kumar, Suman Lata Tripathi, "Implementation of CMOS SRAM Cells in 7,8,10 and 12 Transistor Topologies and theirPerformance," in International Journal of Engineering and Advanced Technology Vol.8, Issue-2S2, Jan- 2019.8. S. Shaik and P. Jonnala, "Performance evaluation of different SRAM topologies using 180, 90 and 45 nm technology," 2013 International Conference on Renewable Energy and Sustainable Energy (ICRESE), Coimbatore, India, 2013, pp. 15-20. https://doi.org/10.1109/ICRESE.2013.6927819

9. F. Moradi and J. K. Madsen, "Improved read and write margins using a novel 8T-SRAM cell," 2014 22nd International Conference on Very Large-Scale Integration (VLSI-SoC), Playa del Carmen, Mexico, 2014, pp. 1-5. https://doi.org/10.1109/VLSI-SoC.2014.7004186

10. Design of 13T SRAM Bitcell in 22nm Technology using Fin FET for Space Applications. (2019). In International Journal of Recent Technology and Engineering (Vol. 8, Issue 2S5, pp. 226–230).. https://doi.org/10.35940/ijrte.b1046.0782s519

11. T. K., R., S. H., M. S. H., & S Y, S. (2023). Performance Evaluation of Different Topologies of SRAM and SRAM Memory Array Design at 180nm Technology. In International Journal of Engineering and Advanced Technology (Vol. 12, Issue 3, pp. 1–10). https://doi.org/10.35940/ijeat.c3983.0212323

12. Dutta, U., Soni, M. K., & Pattanaik, M. (2019). Design and Analysis of Gate All Around Tunnel FET

based SRAM. In International Journal of Innovative Technology and Exploring Engineering (Vol. 8, Issue 9, pp. 1492–1500). https://doi.org/10.35940/ijitee.i8237.078919

13. Kumari, N., & Niranjan, Prof. V. (2022). Low-Power 6T SRAM Cell using 22nm CMOS Technology. In Indian Journal of VLSI Design (Vol. 2, Issue 2, pp. 5–10). https://doi.org/10.54105/ijvlsid.b1210.092222

14. Yadav, P. S., & Jain, H. (2023). Review of 6T SRAM for Embedded Memory Applications. In Indian Journal of VLSI Design (Vol. 3, Issue 1, pp. 24–30). https://doi.org/10.54105/ijvlsid.a1217.033123

AUTHORS PROFILE

M G Srinivasa M. Tech in VLSI and Embedded systems from SJCE, PhD in the field of Wireless Body Area Network (WBAN) for real time wearable physiological parameters monitoring and algorithms to classify health status from Visvesvaraya Technological University Belgaum, under the guidance of Dr. P S Pandian Scientist G LRDE DRDO. Presently working as Associate Professor in the Department of Electronics and Communication Engineering, Maharaja Institute of Technology Thandavapura having 17 years of teaching and 8 years of Industrial experience. Field of interest includes Analog Electronics, Signals & Systems, Linear Integrated Circuits, Antenna and propagation, Digital Signal Processing, and Embedded system design. Actively involved in IETE Professional body activities like workshops seminars national level model & paper presentation contest. Instrumental in signing MOUs with software and hardware companies for the benefit of students in getting Internship training and placements.

Bhavana M.S final-year electronics and communication engineering student at The National Institute of Engineering, Mysuru with a keen interest in VLSI, Analog and Digital Communication, embedded systems and PCB design. Possess a strong academic background and is skilled in Cadence Virtuoso, Verilog coding, ARM Cortex programming, and Vivado. Aspiring to pursue a master's degree in VLSI in USA with a passion for innovative technologies and a track record of excellence. Worked on SAR ADC design for biomedical applications in cadence 180nm technology. Aims to acquire hands-on experience and deep practical expertise in the realm of Semiconductor design particularly in VLSI and related domains.

ISSN: 2249-8958

Aspects of Collinearity Property in Mechanics

Răzvan Bogdan Itu, Mihaela Toderaș

A B S T R A C T

Interdisciplinarity encourages students to make connections between different academic disciplines, fostering a deeper understanding of complex real-world problems. By integrating various subjects, students are able to develop critical thinking skills and apply their knowledge in practical ways. This approach not only enhances their learning experience but also prepares them for the challenges they may face in their future careers. In the paper, a strong connection between mathematics and mechanics has been demonstrated. It is important to note that the discussion of this topic is just scratching the surface of the many aspects that can be explored. This example highlights the principle of continuous learning and the endless possibilities for acquiring new knowledge in any field. The process of knowledge is infinite and always open to new contributions. By integrating knowledge from different disciplines, individuals can gain a holistic understanding of complex concepts and phenomena. This interdisciplinary approach fosters critical thinking skills and encourages creative problem-solving, enabling learners to tackle real-world challenges with a broader perspective. Additionally, the collaboration between disciplines promotes innovation and encourages the development of new ideas and solutions. This paper presents aspects regarding the application of the collinearity property in mechanics. The laws of motion of a rigid body, scalar functions of time are meant, which determine, in any moment of the motion, the position of the body in relation to a benchmarkthrough the examples taken in the study were taken from point kinematics and rigid kinematics, also studying how the velocity and acceleration of the points of the solid body vary, in relation to the same reference system.

Keywords: Collinearity, Kinematic Movement, Velocity.

I. INTRODUCTION

The problem of collinearity has been considered in many studies of applied mechanics carried out by different researchers [6], [8], [10], [11], [18]. Starting from some properties of the Lemaitre regularization [9], Titov studies the problem with three bodies. He applies these properties to the degenerate case of a rectilinear problem in the space of shapes and obtains a number of collinear orbits [13] and also to the degenerate case of an isosceles problem in the space of forms [14]. Applying the collinearity problem, the author obtains a number of collinear orbits, respectively isosceles orbits, whose properties he analyses.

Special results were obtained by Balbiani et al. [1], [2].

Starting from the fact that a geometrical figure is a relation on a finite set of points whose properties can be expressed using equations between terms of the first order, they elaborate a narrowing-based unification algorithm that will solve every system of geometrical equations in the language of affine geometry of collinearity. Advanced research has been carried out by applying the collinearity procedure to the identification of large-scale linear systems using Gaussian regression [17][24]. The authors developed a strategy cast in a Bayesian regularization framework where any impulse response is seen as realization of a zero-mean Gaussian process. Kinematics studies mechanical motion, without taking in consideration forces and moments, that is, it exclusively follows its geometric aspect. Kinematics of the point studies the movement of a material point, irrespective of the causes of this movement. It allows the study of the relationships between the parameters describing the motion and their equations or

or transformations in various systems of coordinates or in the case of a change of a reference system [3], [5], [12]. The movement of a body in relation to a reference system is known, if the motion laws of each point of the body can be determined. By the laws of motion of a rigid body, scalar functions of time are meant, which determine, in any moment of the motion, the position of the body in relation to a benchmark [4], [7], [15]. The movement of a solid rigid body in relation to a fixed reference system is only determined when at any time, the position, velocity and acceleration of any point of the rigid body are known. The fundamental problem of the kinematics of the rigid body lies in establishing the distribution of velocity and acceleration (determination at a certain moment of the set of velocity and acceleration vectors for their various points. In mechanics, especially in kinematics, as in geometry, there are aspects in which reference is made to collinearity property, both in theory, and in applications [16], [17][22][23].

The paper presents different aspects of the collinearity property, the theoretical solution and the applied part.

II. PROBLEM FORMULATION

A. Properties of Velocity Distribution in Rigid Bodies

In the kinematics of rigid bodies, the fundamental problem lies in establishing the distribution of velocity and acceleration. The motion of a rigid body is known when there is the possibility of knowing the movement of any of its points in relation to a certain reference system x1O1y1, assumed to be immobile. Practically, it is neither necessary nor possible for the movement of the rigid body to be described, by the movement of each of its points. Since the hypothesis of rigidity exists, namely the relative distances between the points of the rigid body stay constant, it is sufficient for the exact positions of only some of the points to be known, at any time, from which the positions of the others are determined.

It results that it is useful to consider a reference system xOy solidary with the rigid body, in relation to which the points of the body to be positioned. Similarly, one can also study how the velocity and acceleration of the points of the solid body vary, in relation to the same reference system [19]-[21]. These variation laws for the velocity and acceleration of points, depending on their position inside the solid rigid body (and not depending on time) is called velocity distribution, and acceleration distribution, respectively. These distributions are established starting from expressing the position of a current point M of the solid body in relation to the two reference systems (Fig. 1).

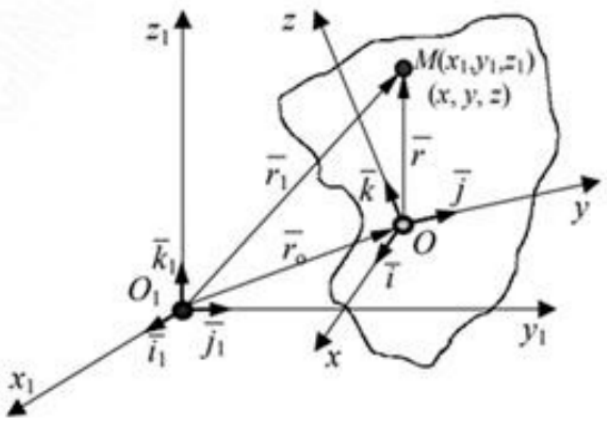

Fig. 1. The Position of the Current Point M of the Solid Body In Relation to the two Reference Systems

Thus, the position vector for point M is written:

$$\begin{aligned}\bar{r}_1(t) &= \bar{r}_0(t) + \bar{r}(t) \\ &= \bar{r}_0(t) + x\bar{i}(t) + y\bar{j}(t) + z\bar{k}(t)\end{aligned} \quad (1)$$

The known coordinates x, y, z of the point stay constant during the motion. The unknown elements of the problem are in this case only the vectorial functions $\bar{r}_0(t)$ (the origin of the mobile system, a system solidary with the rigid body, and which obviously moves alongside with it), and the versor of the axes of the mobile system, $\bar{i}(t), \bar{j}(t), \bar{k}(t)$. Derivation in relation to time of the (1) leads to establishing the velocity of point M in relation to the fixed reference system:

$$\bar{v}_M = \dot{\bar{r}}_1(t) = \dot{\bar{r}}_0(t) + \dot{\bar{r}}(t) \quad (2)$$

The derivative of the position vector of point O in relation to time represents its velocity:

$$\dot{\bar{r}}_0(t) = \bar{v}_0(t) \quad (3)$$

And:

$$\begin{aligned}&\dot{\bar{r}}(t) = x\dot{\bar{i}}(t) + y\dot{\bar{j}}(t) + z\dot{\bar{k}}(t) \\ &\dot{\bar{r}}(t) = x\bar{\omega}\times\bar{i} + y\bar{\omega}\times\bar{j} + z\bar{\omega}\times\bar{k} \\ &\dot{\bar{r}}(t) = \bar{\omega}\times(x\bar{i}) + \bar{\omega}\times(y\bar{j}) + \bar{\omega}\times(z\bar{k}) \\ &\dot{\bar{r}}(t) = \bar{\omega}\times\bar{r}\end{aligned} \quad (4)$$

Since:

$$\dot{x} = 0, \dot{y} = 0, \dot{z} = 0, \dot{\bar{i}} = \bar{\omega}\times\bar{i}, \dot{\bar{j}} = \bar{\omega}\times\bar{j}, \dot{\bar{k}} = \bar{\omega}\times\bar{k}$$

(Poisson equations) and is the angular velocity vector of rotation of the mobile system.
In the end (2) becomes:

$$\bar{v}_M = \bar{v}_0 + \bar{\omega}\times\bar{r} \quad (5)$$

Equation (5) is known as Euler formula for velocity distribution represents in fact the fundamental formula of the kinematics of rigid bodies, and with its help the velocity distribution of the points of rigid bodies is carried out at a given time of their motion. With Euler formula a series of properties can be established of velocity distributions of the points of a solid rigid body found in a general motion.
Without demonstrating those, we shall present in the following, some of the most important properties of the velocity distribution in the general motion of the rigid body.
Vector $\bar{\omega}$ is the same in any point of the rigid body.Vector $\bar{\omega}$ does not depend on the choice of the origin of the mobile reference system that is, $\bar{\omega}$ is an invariant in relation to the axes solidary with the rigid body.The projections of the velocities of two points in the solid body on the line uniting those, are equal and of the same sense: theorem of the velocity projections (Fig. 2).

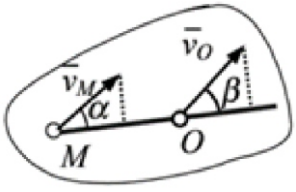

Fig. 2. Velocity Projections

The extremities of the velocity vector of certain collinear points in a solid body in a general motion, are in their turn collinear: theorem of collinearity of velocity vector extremities (Fig. 3).

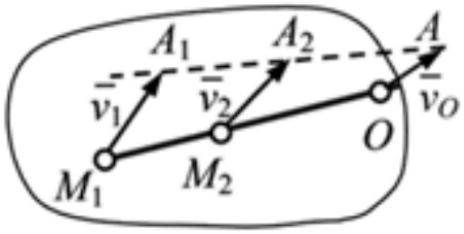

Fig. 3. Example of a Figure Caption (Figure Caption)

Velocity projections of various points of a solid rigid body found in a general motion, in the direction of vector are constant (Fig. 4). For this property the following comments are made[25][26].

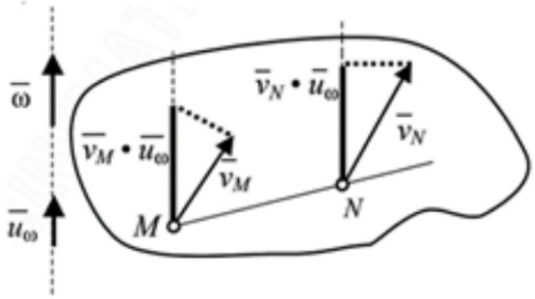

Fig. 4. Velocity Projections on the Line $\bar{\omega}$

This property shows that there are no null velocity points in the general movement of the rigid body. If the vectors and are perpendicular in a point, the property stays valid for all the points of the rigid body. The velocity distribution in the general motion of the rigid body, has a second invariant (scalar invariant), namely, projection of velocityv in the direction of the vector $\bar{\omega}$:

$$v_\omega = \frac{\bar{v} \bullet \bar{\omega}}{|\bar{\omega}|} \qquad (6)$$

The points in a rigid body found in a general motion and which are situated on a line parallel with the direction of the vector $\bar{\omega}$ have the same velocity (Fig. 5).

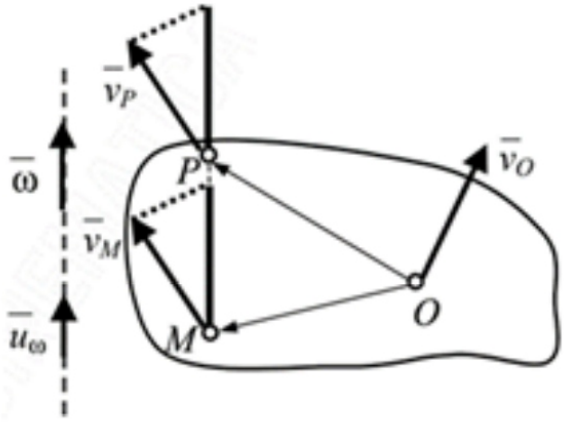

Fig. 5. Points with $\bar{v} \in (\Delta) \| \bar{\omega}$

The property is useful for the study of various particular movements, such as rotational movement, helical movement, etc.

B. Collinearity Property of the Extremities of the Velocity Vectors

The statement of the property (theorem) of collinearity of the extremities of the velocity vectors is: the extremities of the velocity vectors (drawn at the same scale) of three collinear points belonging to a rigid body in motion are collinear as well. Since a vector is characterized by size, direction and sense, having an origin (the point of application of the vector) and an extremity (the latter being generally noted with letters, they being considered as geometric points), the problem leads to demonstrating the collinearity of three points (the extremities of the velocity vectors). In geometry, collinearity is the property of a number greater than two points to belong to the same line. Several non-collinear points are points that cannot belong to the same line. This can be also demonstrated using vectors and complex numbers, as for coplanarity. Out of the methods specific to demonstrate collinearity used in geometry, we mention the following methods:

▪ Demonstration of collinearity with the help of elongated angle (additional angles)

If A and C are situated on either side of line BD, and m(<ABD)+m(<DBC)=180o, then points A, B and C are collinear (Fig. 6).

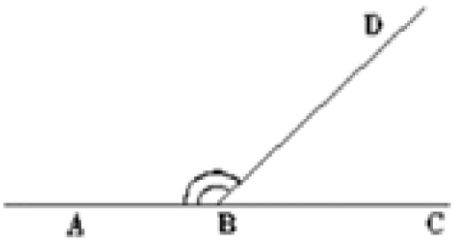

Fig. 6. Additional angles

Demonstration of collinearity using the reciprocal of the theorem of opposite angles at the apex.

If point B is situated on line DE, and A, and C are on either side of line DE, and <ABD = <CBE, then points A, B, C are collinear (Fig. 7).

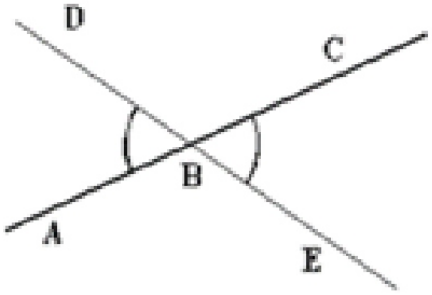

Fig. 7. Angles Opposed at the Peak

▪ Demonstration of collinearity by identifying a line that includes the respective points.

To show that points A, B, C are collinear, a line is identified to which they should belong.

▪The condition of collinearity of three points, A(x1,y1), B(x2,y2), C(x3,y3) is obtained if we stipulate that C(x3,y3) point would verify the equation of line AB, that is:

$$\frac{y_3 - y_1}{y_2 - y_1} = \frac{x_3 - x_1}{x_2 - x_1} \tag{7}$$

The condition of collinearity of the three points can also be written in the form of a determinant:

$$\begin{vmatrix} 1 & x_1 & y_1 \\ 1 & x_2 & y_2 \\ 1 & x_3 & y_3 \end{vmatrix} \tag{8}$$

III. PROBLEM SOLUTION

A. Properties of Velocity Distribution in Rigid Bodies

Two vectors are collinear if they have the same direction. This happens when both vectors are nonnull and their supporting lines are parallel or coincide, in the case when one of the vectors is null. The parallelism of the vectors represents a particular case of their collinearity, which is explicable by the fact that free vectors have no fixed position and can be translated in any point of the plane.

B. Demonstration of Collinearity of Points Using the Applications of Complex Numbers in Geometry

If points A, B, C have respectively zA, zB, zC, affixes, then A, B, C are collinear if and only if

$$(z_B - z_A)/(z_C - z_A) \in \mathbb{R}^*.$$

In the following we intend to demonstrate the property of collinearity of velocity vectors of velocity distribution in the general movement of the rigid body, by approaching different methods of demonstrating collinearity.

Consider the points belonging to a rigid body in movement and collinear M1, M2, and M3 (Fig. 8), which is written vectorially in the form:

$$\overline{M_1M_2} = \lambda \overline{M_1M_3} \tag{9}$$

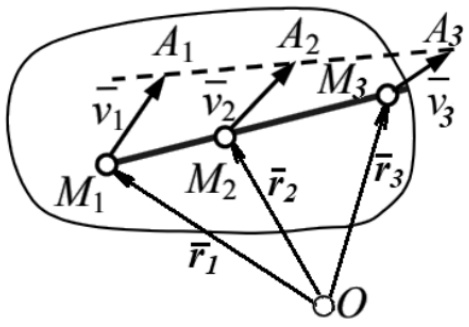

Fig. 8. Schema of Collinearity of Velocity Extremities

At the scale of the drawing, the velocity of points M1, M2 and M3 are:

$$\begin{aligned}\bar{v}_1 &= k\overline{M_1A_1}\\ \bar{v}_2 &= k\overline{M_2A_2}\\ \bar{v}_3 &= k\overline{M_3A_3}\end{aligned} \qquad (10)$$

The proportionality factor k is called the velocity scale. Equation (9), depending on the vectors of position is written in the form:

$$\bar{r}_2 - \bar{r}_1 = \lambda\left(\bar{r}_3 - \bar{r}_1\right) \qquad (11)$$

Deriving the equation (11) in relation to time, considering that $\dot{\bar{r}}_1 = \bar{v}_1, \dot{\bar{r}}_2 = \bar{v}_2, \dot{\bar{r}}_3 = \bar{v}_3$ we get:

$$\bar{v}_2 - \bar{v}_1 = \lambda\left(\bar{v}_3 - \bar{v}_1\right) \qquad (12)$$

At the scale of the drawing, (12) becomes:

$$\overline{M_2A_2} - \overline{M_1A_1} = \lambda\left(\overline{M_3A_3} - \overline{M_1A_1}\right) \qquad (13)$$

Summing up element by element (11) and (13), the following results:

$$\begin{aligned}&\left(\bar{r}_2 + \overline{M_2A_2}\right) - \left(\bar{r}_1 + \overline{M_1A_1}\right) =\\ &\lambda\left[\left(\bar{r}_3 + \overline{M_3A_3}\right) - \left(\bar{r}_1 + \overline{M_1A_1}\right)\right]\end{aligned} \qquad (14)$$

Or:

$$\overline{OA_2} - \overline{OA_1} = \lambda\left(\overline{OA_3} - \overline{OA_1}\right) \qquad (15)$$

Consequently:

$$\overline{A_1A_2} = \lambda\overline{A_1A_3} \qquad (16)$$

wich demonstrates both the collinearity of points A1, A2, A3, and the fact that point A2 divides segment A1A3 in the same ratio in which M2 divides segment M1M3.

The following demonstration of the collinearity theorem of the velocity extremities of three collinear point of a solid rigid body found in a general motion will be done using Euler's formula.

Consider collinear points O, M1, M2 of a solid body and points A, A1, A2 as being the extremities of velocity vectors 0 1 2 v v v , ,(Fig. 3). Considering point O as origin of the mobile system solidary with the rigid body, according to Euler's equation velocities 1 2 v v,have the following equations:

$$\bar{v}_1 = \bar{v}_0 + \bar{\omega}\times\overline{OM_1}, \quad \bar{v}_2 = \bar{v}_0 + \bar{\omega}\times\overline{OM_2} \qquad (17)$$

Where: the position vectors $\overline{OM_1}$ and $\overline{OM_2}$ can be expressed as geometric sums (Fig. 3):

$$\begin{aligned}\overline{OM_1} &= \overline{OA} + \overline{AA_1} + \overline{A_1M} = \bar{v}_O + \overline{AA_1} - \bar{v}_1\\ \overline{OM_2} &= \overline{OA} + \overline{AA_2} + \overline{A_2M} = \bar{v}_O + \overline{AA_2} - \bar{v}_2\end{aligned} \qquad (18)$$

Considering (17), the previous expressions (18) will get the form:

$$\begin{aligned}\overline{OM_1} &= \overline{AA_1} - \bar{\omega}\times\overline{OM_1}\\ \overline{OM_2} &= \overline{AA_2} - \bar{\omega}\times\overline{OM_2}\end{aligned} \tag{19}$$

If the three points O, M_1, M_2 are collinear, then:

$$\overline{OM_1} = \lambda\overline{OM_2} \tag{20}$$

From (19) substituting in (20) the following is inferred:

$$\overline{AA_1} - \bar{\omega}\times\overline{OM_1} = \lambda\left(\overline{AA_2} - \bar{\omega}\times\overline{OM_2}\right) \tag{21}$$

Or:

$$\overline{AA_1} = \lambda\cdot\overline{AA_2} - \bar{\omega}\times\left(\overline{OM_1} - \lambda\cdot\overline{OM_2}\right) \tag{22}$$

But: $\overline{OM_1} - \lambda\cdot\overline{OM_2}$ by virtue of (20). It results $\overline{AA_1} = \lambda\cdot\overline{AA_2}$, that is, the three points A, A_1, A_2 are collinear.

Another method to demonstrate collinearity is the one using vectorial product, knowing that it is annulled when the vectors of the products are collinear. If: $\overline{A_1A_2}\times\overline{A_1A_3} = 0$, then the two vectors are collinear, and the three points A_1, A_2, A_3 respectively, are also collinear. According to Fig. 9 the following equations result:

$$\begin{aligned}&\overline{M_1M_2} + \bar{v}_2 = \bar{v}_1 + \overline{A_1A_2}\\ &\Rightarrow \overline{A_1A_2} = \bar{v}_2 - \bar{v}_1 + \overline{M_1M_2}\\ &\overline{M_1M_3} + \bar{v}_3 = \bar{v}_1 + \overline{A_1A_3}\\ &\Rightarrow \overline{A_1A_3} = \bar{v}_3 - \bar{v}_1 + \overline{M_1M_3}\end{aligned} \tag{23}$$

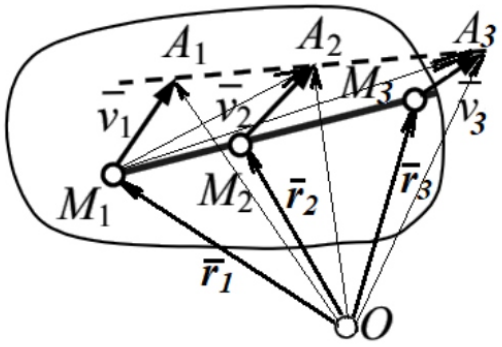

Fig. 9. Schema for Calculation with Vectorial Product

With (23) we have:

$$\overline{A_1A_2}\times\overline{A_1A_3} = \left(\bar{v}_2 - \bar{v}_1 + \overline{M_1M_2}\right)\times\left(\bar{v}_3 - \bar{v}_1 + \overline{M_1M_3}\right) \tag{24}$$

But: $\overline{M_1M_3} = \lambda\overline{M_1M_3} \Leftrightarrow \bar{r}_3 - \bar{r}_1 = \lambda\left(\bar{r}_2 - \bar{r}_1\right) \underset{\Rightarrow}{(\,)'} \bar{v}_3 - \bar{v}_1 = \lambda\left(\bar{v}_2 - \bar{v}_1\right)$

and (24) becomes:

$$\begin{aligned}&\overline{A_1A_2}\times\overline{A_1A_3} = \left(\bar{v}_2 - \bar{v}_1 + \overline{M_1M_2}\right)\times\left[\lambda\left(\bar{v}_3 - \bar{v}_1\right) + \lambda\overline{M_1M_2}\right]\\ &= \left(\bar{v}_2 - \bar{v}_1 + \overline{M_1M_2}\right)\times\lambda\left(\bar{v}_2 - \bar{v}_1 + \overline{M_1M_2}\right) \equiv 0\end{aligned} \tag{25}$$

Thus, the three points A1, A2, A3 are also collinear.

C. Collinearity Condition of three Points Moving on different Trajectories

▪ Applying the property of collinearity.
In the following we shall present an application in which the collinearity principle is used.

The following problem is considered: in the same moment and from the same point O, three bodies are launched in a gravitational field, with different initiated velocities v1, v2, v3represented in Fig. 10.

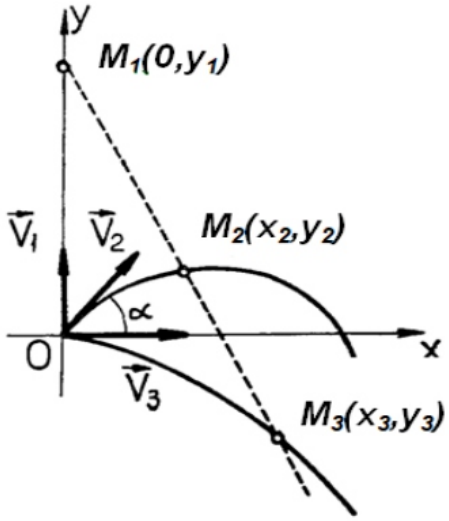

Fig. 10. Launching Points

We aim to find the relationship that should exist between the magnitudes of initial velocities and angle α, so that all along the motion, the three bodies would remain collinear. In order to solve such a collinearity problem, we should admit the following two simplifying hypotheses, which have not been included in its statement: ignoring the air resistance and considering the three bodies as material points. To establish the collinearity condition of the three material points, M1(0,y1), M2(x2,y2) and M3(x3,y3), we appeal at first to our knowledge of analytical geometry. The collinearity condition lies in the following equation according to (8):

$$\delta = \begin{vmatrix} 0 & y_1 & 1 \\ x_2 & y_2 & 1 \\ x_3 & y_3 & 1 \end{vmatrix} \qquad (26)$$

To express the coordinates of points M1, M2 and M3 at any time t > 0, calculated from the moment of launching the bodies, we appeal to our knowledge of kinematics from mechanics:

- vertical throwing up:

$$x_1 = 0, \quad y_1 = v_1 t - \frac{g}{2} t^2 \qquad (27)$$

- obliquely throwing:

$$x_2 = v_2 t \cos\alpha$$

$$y_2 = v_2 t \sin\alpha - \frac{g}{2} t^2 \qquad (28)$$

- horizontally throwing:

$$x_3 = v_3 t, \quad y_3 = -\frac{g}{2}t^2 \tag{29}$$

Substituting then (27), (28) and (29) in determinant (26) we get:

$$\delta = \begin{vmatrix} 0 & v_1 t - \frac{g}{2}t^2 & 1 \\ v_2 \cos\alpha & v_2 t \sin\alpha - \frac{g}{2}t^2 & 1 \\ v_3 t & -\frac{g}{2}t^2 & 1 \end{vmatrix} \tag{30}$$

so that the development of this determinant leads to the required condition:

$$\begin{aligned} & v_3 t\left(v_1 t - \frac{g}{2}t^2\right) = \frac{g}{2}v_2 t^3 \cos\alpha - v_3 t\left(v_2 t \sin\alpha - \frac{g}{2}t^2\right) \\ & -v_2 t \cos\alpha \cdot \left(v_1 t - \frac{g}{2}t^2\right) = 0 \end{aligned} \tag{31}$$

After reducing the similar terms and dividing by t_2, ($t > 0$), we get in the end the equation searched:

$$v_2 v_3 \sin\alpha + v_1 v_2 \cos\alpha - v_1 v_3 = 0 \tag{32}$$

- Demonstration of collinearity of the points using vectors.

We shall further demonstrate the collinearity of the points using vectors this time. Vectors $\bar{r}_A = (x_A, y_A)$ and $\bar{r}_B = (x_B, y_B)$ are collinear if and only if their coordinates (projections on axes) are proportional, namely:

$$\frac{x_A}{x_B} = \frac{y_A}{y_B} \tag{33}$$

If: $x_B, y_B \neq 0$, points A, B, C are collinear if and only if vectors $\overline{AB}$ and $\overline{AC}$ are collinear that is, if and only if exists, so that:

$$\overline{AB} = \alpha \overline{AC} \tag{34}$$

But:

$$\begin{aligned} & \overline{AB} = \alpha \overline{AC} \quad \Leftrightarrow \quad (x_B - x_A)\bar{i} + (y_B - y_A)\bar{j} \\ & = (\alpha x_C - \alpha x_A)\bar{i} + (\alpha y_C - \alpha y_A)\bar{j} \\ & \Leftrightarrow (x_B - x_A) = \alpha(x_C - x_A) \\ & (y_B - y_A) = \alpha(y_C - y_A) \\ & \Leftrightarrow \frac{x_B - x_A}{x_C - x_A} = \frac{y_B - y_A}{y_C - y_A} \\ & with: x_C - x_A \neq 0, y_C - y_A \end{aligned} \tag{35}$$

Thus, according to Fig. 11, for points M1, M2 and M3 we have:

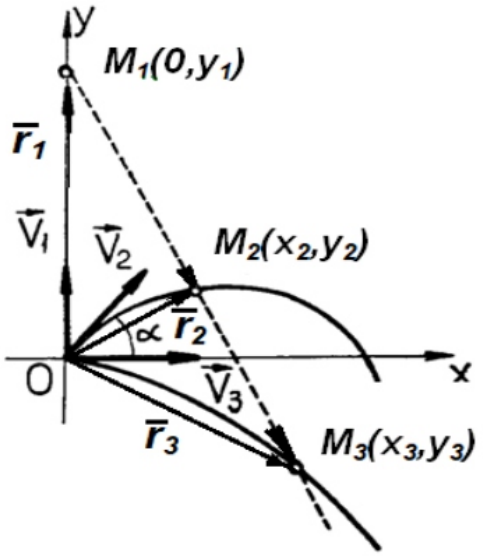

Fig. 11. Position Vectors of Points

$$\bar{r}_1 = 0\bar{i} + y_1\bar{j},\ \ \bar{r}_1 = \left(v_t t - \frac{g}{2}t^2\right)\bar{j}$$

$$\bar{r}_2 = x_2\bar{i} + y_2\bar{j},\ \ \bar{r}_2 = v_2 t\cos\alpha\,\bar{i} + \left(v_2 t\sin\alpha - \frac{g}{2}t^2\right)\bar{j} \qquad (36)$$

$$\bar{r}_3 = x_3\bar{i} + y_3\bar{j},\ \ \bar{r}_3 = v_3 t\bar{i} + \left(-\frac{g}{2}t^2\right)\bar{j}$$

For points M_1, M_2 and M_3 to be collinear the condition is:

$$\overline{M_1M_3} = \alpha\overline{M_1M_2} \quad or \quad \frac{x_3 - x_1}{x_2 - x_1} = \frac{y_3 - y_1}{y_2 - y_1} \qquad (37)$$

Thus, it results:

$$\frac{v_3 t}{v_2 t\cos\alpha} = \frac{v_1 t}{-\left(v_2 t\sin\alpha - v_1 t\right)} \Rightarrow \quad -v_3 v_2\sin\alpha + v_3 v_1 = v_1 v_2\cos\alpha \qquad (38)$$

It is noticed that (37) is identical to (31).

▪ Determining the collinearity relationship of three points using complex numbers.

Next, we shall determine the collinearity equation for points M1, M2 and M3 using complex numbers. Associating z = x + iy, M(x, y) to set R of real numbers, Ox axis corresponds, called in this context, the real axis, and to set iRof imaginary numbers, axis Oy, called imaginary axis. The plane the points of which are identified with complex numbers by function g o f, previously defined, is called complex plane. Affixes of points M1, M2 and M3 (fig. 12) are z1, z2, z3. Points M1(z1), M2(z2) and M3(z3) are collinear if and only if (z3-z1)/(z3-z2) belongs to R.

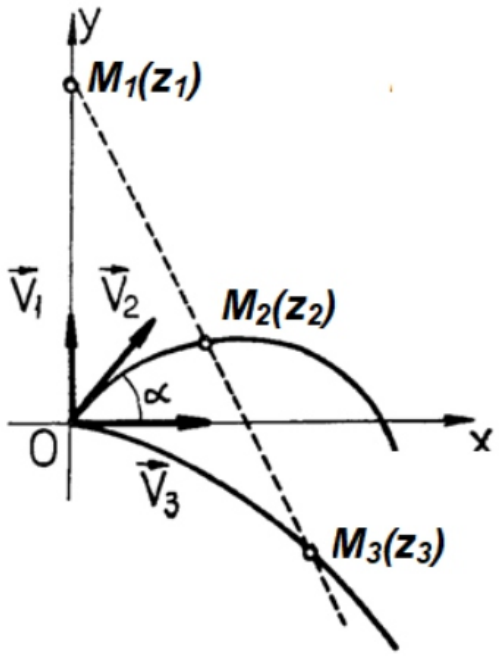

Fig. 12. Affixes of Points M_1, M_2 and M_3

According to Fig. 12 and the kinematic equations from mechanics, we have:

$$z_1 = x_1 + iy_1, \quad z_1 = i\left(v_1 t - \frac{g}{2}t^2\right)$$

$$z_2 = x_2 + iy_2, z_2 = v_2 t\cos\alpha + i\left(v_2 t\sin\alpha - \frac{g}{2}t^2\right) \qquad (39)$$

$$z_3 = x_3 + iy_3, \quad z_3 = v_3 t + i\left(-\frac{g}{2}t^2\right)$$

$$\frac{z_3 - z_1}{z_2 - z_1} = \frac{x_3 + iy_3 - (x_1 + iy_1)}{x_2 + iy_2 - (x_1 + iy_1)} = \frac{x_3 - x_1 + i(y_3 - y_1)}{x_2 - x_1 + i(y_2 - y_1)}$$

$$\Leftrightarrow \frac{v_3 t - 0 + i\left(-\frac{g}{2}t^2 - v_1 t + \frac{g}{2}t^2\right)}{v_2 t\cos\alpha - 0 + i\left(v_2 t\sin\alpha - \frac{g}{2}t^2 - v_1 t + \frac{g}{2}t^2\right)} \qquad (40)$$

$$= \frac{v_3 t - iv_1 t}{v_2 t\cos\alpha + i(v_2 t\sin\alpha - v_1 t)} = \lambda$$

Where: $\lambda \in \mathbb{R}^*$.

Thus, we shall have:

$$\frac{v_3 t - iv_1 t}{v_2 t\cos\alpha + i(v_2 t\sin\alpha - v_1 t)} = \lambda$$

$$\left\{v_3 t - iv_1 t = \lambda\left[v_2 t\cos\alpha + i(v_2 t\sin\alpha - v_1 t)\right]\right\}\frac{1}{t} \qquad (41)$$

$$v_3 - \lambda v_2 \cos\alpha = i\left[v_1 + \lambda\left(v_2 \sin\alpha - v_1\right)\right]$$

$$v_3 - \lambda v_2 \cos\alpha - i\left[v_1 + \lambda\left(v_2 \sin\alpha - v_1\right)\right] = 0$$

For the last equation of (40) to be $v_3 - \lambda v_2 \cos\alpha - i\left[v_1 + \lambda\left(v_2 \sin\alpha - v_1\right)\right] = 0$ we must have: $v_3 - \lambda v_2 \cos\alpha = 0$ and $v_1 + \lambda\left(v_2 \sin\alpha - v_1\right) = 0$, whence:

$$\lambda = \frac{v_3}{v_2 \cos\alpha} \quad and \quad \lambda = \frac{v_1}{v_1 - v_2 \sin\alpha} \tag{42}$$

Equalizing the two equations of (42), it results:

$$\frac{v_3}{v_2 \cos\alpha} = \frac{v_1}{v_1 - v_2 \sin\alpha} \Rightarrow \quad v_3\left(v_1 - v_2 \sin\alpha\right) = v_1 v_2 \cos\alpha \tag{43}$$

Equation (42) is identical with (32).

▪ Determination of collinearity by means of the elongated angle.

We shall further consider the demonstration of collinearity with the help of the elongated angle (additional angles). If M1and M3 are situated on one side and the other of line OM2 and m(<M1M2O) + m(<OM2M3) = 180° (Fig. 13), then points M1, M2 and M3 are collinear.

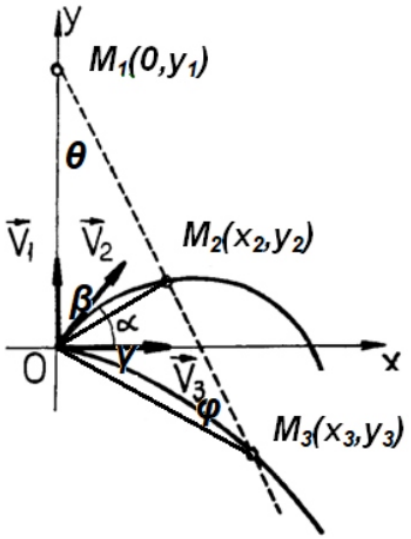

Fig. 13. Case of Elongated Angle

Taking into consideration Fig. 13, we shall make the following notations:

$$\sphericalangle OM_1M_2 = \theta, \quad \sphericalangle M_1OM_2 = \beta$$
$$\sphericalangle OM_3M_2 = \varphi, \quad \sphericalangle M_2OM_3 = \gamma \tag{44}$$

From ΔOM_1M_2 results that:

$$\sphericalangle OM_2M_1 = 180^0 - \left(\beta + \theta\right) \tag{45}$$

From ΔOM_3M_2 results that:

$$\sphericalangle OM_2M_3 = 180^0 - \left(\gamma + \varphi\right) \tag{46}$$

Calculating the sum of the extent of angles $\sphericalangle OM_2M_1$ and $\sphericalangle OM_2M_3$, we get:

$$\sphericalangle OM_2M_1 + \sphericalangle OM_2M_3 = 180^0 - (\gamma + \varphi) + 180^0 - (\beta + \theta) = 360^0 - (\gamma + \varphi + \beta + \theta) \quad (47)$$

But:

$$(\gamma + \varphi + \beta + \theta) = 180^0 \quad (48)$$

Equation (47) becomes:

$$\sphericalangle OM_2M_1 + \sphericalangle OM_2M_3 = 180^0 \quad (49)$$

Whence it results that points M_1, M_2 and M_3 are collinear and then the vectors $\overline{M_1M_2}$ and $\overline{M_1M_3}$ being collinear, their vectorial product is null. Thus, we have:

$$\overline{M_1M_2} \times \overline{M_1M_3} = \left[v_2 t \cos\alpha \bar{i} - (v_2 t \sin\alpha - v_1 t) \bar{j} \right] \times (v_3 t \bar{i} + v_1 t \bar{j}) \quad (50)$$

$$= \begin{vmatrix} \bar{i} & \bar{j} & \bar{k} \\ v_2 t \cos\alpha & v_1 t - v_2 t \sin\alpha & 0 \\ v_3 t & v_1 t & 0 \end{vmatrix} = 0$$

From the development of the determinant, we get:

$$v_2 v_3 \sin\alpha + v_1 v_2 \cos\alpha - v_1 v_3 = 0 \quad (51)$$

Equation (51) being identical with equation (32). Such an issue lends itself to interesting discussions. Obviously, collinearity is not possible if condition (32) is not met, and which, as it is noticed, has a certain symmetry. Moreover, it is noticed that the disposition of the velocities of the three bodies is symmetrical in relation to axis Oy, the result (32) remaining. In this context, other dispositions of velocities of the three bodies can be looked for, in order to meet the condition of collinearity, if not all along the motion, at least for certain moments considered in relation to the moment of simultaneous launching of the bodies.

Next, we shall limit ourselves only to the condition (32), assuming v1, v2, v3 being given, and trying to determine α, for which collinearity is maintained. To this end, we must solve equation (32) in relation to the unknown α.

By working out this equation, we shall express $\sin\alpha$ and $\cos\alpha$ by $x = tg(\alpha/2)$:

$$\sin\alpha = \frac{2x}{1+x^2}, \quad \cos\alpha = \frac{1-x^2}{1+x^2} \quad (52)$$

Substituting (52) in (32) we get the algebraic equation of the form:

$$v_1 (v_2 + v_3) x^2 + 2 v_2 v_3 x - v_1 (v_2 - v_3) = 0 \quad (53)$$

Equation (53) has real solutions insofar as its discriminant $\Delta \geq 0$, that is, insofar as:

$$v_2^2 v_3^2 + v_1^2 (v_2^2 - v_3^2) \geq 0 \quad (54)$$

In this case, the solutions for (53) are:

$$x_{1,2} = \frac{-v_2 v_3 \pm \sqrt{v_2^2 v_3^2 + v_1^2\left(v_2^2 - v_3^2\right)}}{v_1\left(v_2 + v_3\right)} \quad (55)$$

Remaining only in the first quadrant of the system xOy, $\alpha \in (0, \pi/2)$, the only possible solution for x is:

$$x = x_1 = \frac{\sqrt{v_2^2 v_3^2 + v_1^2\left(v_2^2 - v_3^2\right)} - v_2 v_3}{v_1\left(v_2 + v_3\right)} \quad (56)$$

Obviously, the solution (56) is acceptable if $v_2 > v_3$ and, as a result:

$$\alpha = 2arctgx$$

$$\alpha = 2arctg\frac{\sqrt{v_2^2 v_3^2 + v_1^2\left(v_2^2 - v_3^2\right)} - v_2 v_3}{v_1\left(v_2 + v_3\right)} \quad (57)$$

IV. CONCLUSION

Interdisciplinarity is a cooperation between various disciplines of the same curricular area, regarding a certain phenomenon, process, the complexity of which can be demonstrated, explained, solved, only by the action of several factors. Interdisciplinarity involves approaching the complex contents with the aim of forming a unitary image on a certain subject matter. This implies combining two or several academic disciplines in one single activity. Thus, new knowledge is accumulated in several fields simultaneously. Mechanics depends on mathematics, and we can realize this by the fact that we cannot solve any problem of mechanics without mathematics.

In the paper the tight connection between the two fundamental disciplines has been shown, mathematics and mechanics. For the time being, stopping here with the discussion of the problem, we should mention that such a discussion is far from exhausting the multitude of aspects that can be raised. This is a small example supporting the principle of continuity of knowledge, of the fact that the process of knowledge is unlimited, and as in any science, it stays open all the time for acquiring new contributions.

DECLARATION STATEMENT

Funding	No, we did not receive.
Conflicts of Interest	No conflicts of interest to the best of our knowledge.
Ethical Approval and Consent to Participate	No, the article does not require ethical approval and consent to participate with evidence.
Availability of Data and Material	Not relevant.
Authors Contributions	All authors have equal participation in this article.

REFERENCES

1. P. Balbiani, L.F. del Cerro, "Affine geometry of collinearity and conditional term rewriting". In: Comon, H., Jounnaud, JP. (eds) Term Rewriting. TCS School 1993. Lecture Notes in Computer Science, vol 909. Springer, Berlin, Heidelberg, 1995,https://doi.org/10.1007/3-540-59340-3_14.

2. P. Balbiani, V. Dugat, L. Fariñas del Cerro, A. Lopez, Eléments de géométrie mécanique. Hermès, Paris, France, 1994.
3. P. Bratu, Mecanică teoretică, IMPULS Publishing House, București, 2006.
4. Collinear Vectors: Definition, Condition, Formula with Proof. Available: https://testbook.com/maths/collinear-vectors.
5. H.S.M. Coxeter, S.L. Greitzer, Collinearity and Concurrence. Geometry Revisited. Washington, DC: Math. Assoc. Amer., 1967, pp. 51-79. ch. 3.
6. De Marco P Júnior, C.C. Nóbrega, Evaluating collinearity effects on species distribution models: An approach based on virtual species simulation. PLoS ONE 13(9): e0202403, 2018,https://doi.org/10.1371/journal.pone.0202403
7. G.A. Dirac, Collinearity Properties of sets of points, The Quarterly Journal of Mathematics, Volume 2, Issue 1, 1951, pp. 221–227, https://doi.org/10.1093/qmath/2.1.221
8. I.Love, The symmetry properties and collinearity of the magnetogyric, hyperfine splitting and magnetic susceptibility tensors, Molecular Physics, 30:4, 1975, 1217-1220, DOI: 10.1080/00268977500102761
9. G. Lemaître, "Regularization of the three-body problem", Vistas in Astronomy, Volume 1, 1955, p. 207-215, https://doi.org/10.1016/0083-6656(55)90028-3.
10. C. H. Mason, W. D. Perreault, Collinearity, Power, and Interpretation of Multiple Regression Analysis. Journal of Marketing Research, 28(3), 1991, p. 268–280. https://doi.org/10.2307/3172863 .
11. R. Nisbet, G. Miner, K. Yale, "Numerical Prediction", Editor(s): Robert Nisbet, Gary Miner, Ken Yale, Handbook of Statistical Analysis and Data Mining Applications, 2nd ed. Academic Press, 2018, p 187-213, ch.10. https://doi.org/10.1016/B978-0-12-416632-5.00010-4.
12. R. Sfichi, Caleidoscop de fizică, Albatros Publishing House, București, 1988.
13. V. Titov, Some properties of Lemaitre regularization. II isosceles trajectories and figure-eight, Astronomische Nachrichten, 10.1002/asna.202114006, 343, 3, 2021.b.
14. V. Titov, Some properties of Lemaitre regularization: Collinear trajectories. Astronomische Nachrichten, 342, 3, 2021.a.
15. R. Voinea, D. Voiculescu, V. Ceauşu, Mecanică. 2nd ed. E.D.P., București, 1983.
16. E.W. Weisstein, Collinear. From MathWorld-A Wolfram Web Resource. Available: https://mathworld.wolfram.com/Collinear.html
17. C. Wenqi, G. Pillonetto, Dealing with Collinearity in Large-Scale Linear System Identification Using Gaussian Regression. arXiv:2302.10959 [stat.ML] Machine Learning (stat.ML). Cornell University. 2023. https://doi.org/10.48550/arXiv.2302.10959
18. R.R. Wilcox, Robust Regression, Editor(s): Rand R. Wilcox, Introduction to Robust Estimation and Hypothesis Testing (Fifth Edition), Academic Press, 2022, pp. 577-651, ch.10.https://doi.org/10.1016/B978-0-12-820098-8.00016-6 .
19. https://www.preferatele.com/docs/matematica/1/interpretarea-geomet16.php
20. https://www.scritub.com/stiinta/matematica/
21. https://smartician.ro/interdisciplinaritatea-sau-care-sunt-prietenii-matematicii/
22. Abdel-Wahab, A. M. (2020). Experimental Work for Evaluation the Time Saving Between Different GPS Techniques for Makkah- Jeddah Region. In International Journal of Innovative Technology and Exploring Engineering (Vol. 9, Issue 9, pp. 313–324). https://doi.org/10.35940/ijitee.i7206.079920
23. Aswal, P., Singh, R., kumar, R., Bhatt, A., & Raj, T. (2020). Resolving the four – Bar Link Mechanism by Kinamatics and Revolving Angle Solution. In International Journal of Recent Technology and Engineering (IJRTE) (Vol. 8, Issue 5, pp. 1003–1009). https://doi.org/10.35940/ijrte.e6069.018520
24. Rizvi, Dr. S. S. H. (2019). Isomorphism and Automorphism in Closed Kinematic Chains. In

International Journal of Engineering and Advanced Technology (Vol. 8, Issue 6, pp. 2457–2460). https://doi.org/10.35940/ijeat.f8547.088619

25. Ganesh, Dr. E. N. (2022). Analysis of Velocity Measurement of Radar Signal in Space Vehicle Application using VLSI Chip. In Indian Journal of VLSI Design (Vol. 2, Issue 1, pp. 16–20). https://doi.org/10.54105/ijvlsid.c1207.031322

26. Mustofa, B., & Hidayah, R. (2020). The Effect of on-Street Parking on Vehicle Velocity and Level of Service at Cik Di Tiro Street Yogyakarta. In International Journal of Management and Humanities (Vol. 4, Issue 5, pp. 99–102). https://doi.org/10.35940/ijmh.e0534.014520

AUTHORS PROFILE

Lecturer Itu Razvan Bogdan, at University of Petroşani, Faculty of Mechanical and Electrical Engineering, Department of Mechanical, Industrial and Transportation Engineering, Romania. Graduate Engineer - Engineering and Environmental Protection in Industry at University of Petroşani, Faculty of Mine and Machine Building Technology at University of Petroşani, Faculty of Mechanical and Electrical Engineering. În the 10-th years of scientific and didactic activity, I have elaborated, supported and published as an author or coauthor in various groups, a number of over 70 scientific papers in national and international jurnals and conferences and autor of 8 books in the feeld of mechanics, material strengh, machine part, green design, etc.

Professor Toderas Mihaela, PhD supervisor in Mines, Oil and Gas (Dr. habil.) at University of Petroşani, Faculty of Mines, Romania. Research Area: Underground and quarries mineral resources exploitation, stability and reliability of underground works mining, Geomechanics, Rock Mechanics and Rock Rheology. Author of 16 books, of which 3 books published in international publishing houses; Author of 9 international book chapters; 127 scientific papers published in international scientific journals, as well national and international conferences; National and International grant manager and research team member (more than 110); 2 Article-type research results award. Any other remarkable point(s): Expert Engineer in Technical, Economic and Management of Mining Companies, title obtained after graduating National Polytechnic Institute of Loraine, Nancy – France; Member in the following professional organizations: International Association of Engineering Geology (IAEG), Romanian Association of Engineering Geology (ARGI), International Society for Soil Mechanics and Geotechnical Engineering (ISSMGE), Romanian Society for Soil Mechanics and Geotechnical Engineering (SRGF), General Association of Engineers from Romania (AGIR); Reviewer and member of scientific committee of different international conferences; Reviewer member of journals: Sustainability, Axioms, Minerals, Energies, Mathematics, Processes; JMSE; Mining Revue, Proceedings of the Romanian Academy, Journal of Geological Resource and Engineering; Journal of Scientific Research and Reports; International Journal of Environment and Climate Change;

International Research Journal of Public and Environmental Health; Current Journal of Applied Science and Technology; Asian Journal of Geological Research; Journal of Scientific Research and Reports; Asian Basic and Applied Research Journal; Asian Journal of Pure and Applied Mathematics; Asian Journal of Research in Computer Science; Asian Research Journal of Mathematics; Current Journal of Applied Science and Technology.

ISSN: 2249-8958

Enhanced Medical Image Segmentation using Transfer Learning with Res101_UNet: Experimental Insights and Comparative Performance Analysis

D D V Sivaram Rolangi, D. Lalitha Bhaskari

ABSTRACT

Throughout the past few decades, artificial intelligence and machine learning have seen a lot of active research in areas such as computer vision, natural language processing, and speech processing. As a result, deep learning models became state-of-the-art for computer vision tasks such as object detection, classification, segmentation, and other allied tasks. Of course, the fruits of this research are extended to the design of robust and reliable digital health systems as well as other applications in the healthcare sector. Many clinical applications require the automatic segmentation of medical images. Recent deep learning-based approaches have demonstrated state-of-the-art performance in medical image segmentation tasks. In addition to their ability to automatically extract features and generalize over large amounts of data, transfer learning based deep learning models have proven to be handy for data scared areas like medical domains. In this research, we investigate and demonstrate the efficacy of a DCNN-based transfer learning model -Res101_Unet, which has been trained and/or fine-tuned to execute tumor tissue segmentation tasks in MRI, CT, PET, and X-RAY pictures of medical organ scans with little data. For ourexperimental study, we employed two image datasets: 'LiverTumor' and 'Gland Colon Cancer', both obtained from the Kaggleportal. This experimental setup includes an Open-Sourcesegmentation model API. Our findings indicate that domainsimilarity-based transfer learning can be used to data-scarcesectors. We achieved 98.47% accuracy and a IoU score of 0.9891on Liver Tumor data and 0.6956 accuracy and a IoU score of0.7043 on gland colon dataset.

Keywords: Medical Image Segmentation, Deep Learning, ResUnet, DCNN, Transfer learning, Domain Similarity

I. INTRODUCTION

Over the past few decades, we have witnessed a substantial increase in the development of new imaging modalities and their applications to a variety of clinical and biomedical problems. As a result of the huge progress made in some of these technologies, the development of image-based technologies, as well as their use in new fields of research and clinical practice, is gaining momentum and is expected to continue. Image segmentation is key to applying imaging technology to the treatment of many biomedical problems.

It is often necessary to segment and isolate tissues, cells, and organs from two-dimensional or three-dimensional digital image data to conduct subsequent quantitative analysis in a variety of experimental biological studies and clinical medicine. For example, MRI brain scans can be utilized to quantify gray matter and white matter tissues to study neurological disorders (e.g., Alzheimer's), and images can be used to segment cells and tissues in histopathology images to aid in diagnosing different lesions or to characterize the distribution of different cells and tissues.

Thanks to the vastly improved capabilities of imaging, As a result of recent technological advancements, segmentation by hand is no longer a viable option for many quantitative studies [5]. The most important part of medical image processing is image segmentation. Image segmentation is a procedure for

extracting the region of interest (ROI) through an automatic or semi-automatic process.

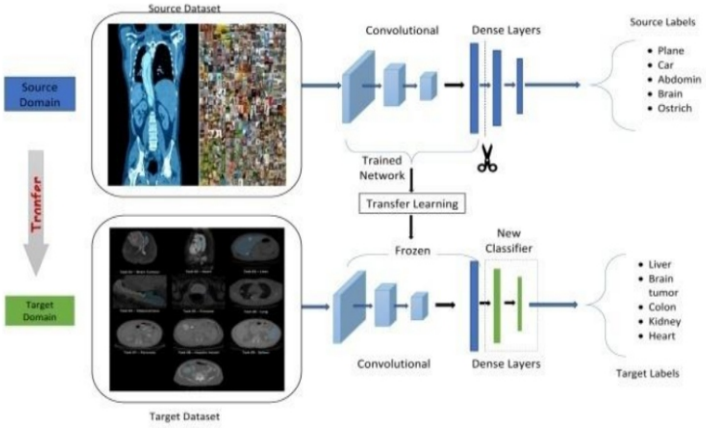

Fig. 1: An Example of Transfer Learning for Medical Image Classification

The deep learning vision algorithms are mostly inspired by human brains. However, they require a huge amount of training examples to learn a new model from scratch and failed to apply knowledge learned from previous domains or tasks [1].

State-of-the-art deep learning models have been proposed in the literature for medical image segmentation tasks like Unet [2], Segnet [3], DRINet [4], etc. The models are either task-specific or domain-specific and need huge data for training and evaluation of these models. In most cases, these models cannot be applied directly to data scared image segmentation. There is a need for a system that can perform segmentation tasks with limited data. Researchers have addressed the above problem and discovered that transfer learning-based approaches are good at generalizing segmentation tasks. Describe what transfer learning is in the next section and the use of transfer learning in medical image segmentation and few of the related work done to date.

The remaining paper is organized as follows: Section I overview of transfer learning and its types, Section II summarizes studies that have attempted to predict and address issues related to Image segmentation using Transfer Learning,Section III gives an overview of the methodology adopted by Res101_Unet, Section IV outlines the datasets, Section V describes the experimental setup based on the segmentation models API, Section VI presents the results, and Section VII concludes the paper and Section VIII mentions the acknoledgements.

II. TRANSFER LEARNING

A. What is Transfer Learning?

Transfer learning is an approach that applies knowledge obtained from one problem (Problem S) to solve another problem (Problem T). The basic idea behind transfer learning is that “Learning to segment a scenery image helps a model later to learn more quickly to segment a biomedical image”.Below is a brief summary of various transfer learning methodologies.

Table. 1: Types of Transfer Learning Methodologies

Transfer Learning Approach	Description	Application	Advantage	Disadvantage
Homogeneous Transfer Learning	Same feature and label space.	Image classification, text classification.	Preserves task structure.	Need source and target tasks are should be related.
Heterogeneous Transfer Learning	Different feature or label space.	Object detection, sentiment analysis.	Allows adaptation to diverse tasks.	Requires alignment of different feature spaces.
Instance-based Transfer Learning	Instance-level knowledge transfer.	Domain adaptation, few-shot learning.	Flexibility in adapting to specific instances.	May suffer from domain shift.
Parameter-based Transfer Learning	Reuse parameters for initialization	Fine-tuning pre-trained models, transfer learning in deep neural networks.	Efficient transfer of learned representations.	Prone to forgetting previously learned tasks.
Relational-based Transfer Learning	Capture task relationships for learning.	Multi-task learning, meta-learning.	Encodes inter-task dependencies.	Complex to model relationships accurately.

It is difficult to gather sufficient medical data for training a segmentation model for medical images. Several researchers have applied the state-of-the-art models built on the ImageNet [6] dataset and other publicly available medical datasets to this task, relying on transfer learning. Therefore, the weights of the task-specific models can be used to train the generalized models.

B. Related Work

A de facto Method for deep learning in medical imaging is to transfer data from natural image datasets, especially those in IMAGENET, using pre-trained weights and standard models. According to Raghu et al [7], transfer learning benefits large models more than small ones. Wang et al. proposed a cross-tissue/organ segmentation method based on the transfer learning method and a modified deep residual U-Net model, which transferred the knowledge of ultrasound image segmentation from one tissue/organ to another [12].

Transfer learning has shown significant promise in improving biomedical image segmentation models. Studies have demonstrated the effectiveness of transfer learning in enhancing segmentation performance across different medical centers and datasets. By fine-tuning pre-trained models with specific data, transfer learning can adapt deep learning models to new image domains, reducing training time and improving segmentation accuracy [13]. Additionally, the development of Scalable and Transferable U-Net (STU-Net) models has further advanced the field, with parameter sizes ranging from 14 million to 1.4 billion. These large-scale models trained on extensive datasets have shown improved transfer capacities and performance gains in medical image segmentation tasks [13]. The utilization of transfer learning and large-scale models underscores their importance in enhancing the accuracy and efficiency of biomedical image segmentation processes.

Liang et al. conducted a large-scale evaluation on the transferability of models pre-trained on the iNat2021 dataset and 14 top self-supervised ImageNet models on 7 diverse medical tasks in comparison with the supervised ImageNet model and found that fine-grained data and self-supervised models are effective for medical image analysis [14].

Nampalle et al. present a transfer learning-based architecture for medical picture segmentation, with ResNet-110 as the backbone network. To improve segmentation accuracy, the authors apply the Tversky similarity loss function. The proposed system is tested on a variety of medical picture datasets, and the findings reveal that transfer learning greatly enhances segmentation performance [15].

Karimi D et al. investigate the dynamics of model parameters and learned representations in transfer learning-based medical image segmentation. The authors employ a U-Net design using ResNet-50 as its backbone network.

The findings indicate that transfer learning enhances segmentation performance by allowing the model

to acquire more robust and generalizable features [16].

Ghavami et al. apply transfer learning to develop a U-Net architecture for biomedical picture segmentation. The authors employ ResNet-50 as the backbone network and test its performance on many biomedical imaging datasets. The results reveal that transfer learning greatly improves segmentation performance over a model built from scratch [17].

Poudel et al. investigate the use of vision-language models (VLMs) for medical picture segmentation using transfer learning. The authors test a U-Net architecture with ResNet-50 as the backbone network on many 2D medical image datasets. The findings indicate that transfer learning from natural to medical images greatly enhances segmentation accuracy, with the extra effect of verbal instructions during finetuning potentially limited [18].

Dorothy Cheng et al. propose a transfer learning-based U-Net architecture for lung ultrasound segmentation. The authors develop the U-Net (V-Unet) using a pre-trained VGG16 model and train it with a grayscale natural salient object dataset (X-Unet). The results reveal that transfer learning greatly improves segmentation performance, while partial-frozen network fine-tuning improves it even more [19][20][21][22][23][24].

These related studies emphasize the importance of transfer learning in medical picture segmentation with ResNet-based architectures. They also demonstrate how transfer learning improves segmentation performance by allowing the model to acquire more robust and generalizable features.

III. METHODOLOGY

The proposed methodology falls under Parameter-based Transfer Learning which includes a deep neural architectural model that is essentially combined with deep 101-layer Resnet [11] for feature extraction and serves as an encoder part, and the traditional Unet [2] is used as a decoder part for up sampling the segmented image using the precise spatial information obtained from the encoder part via skip connections. The following figure depicts the transfer learning methodology used in this experimental study.

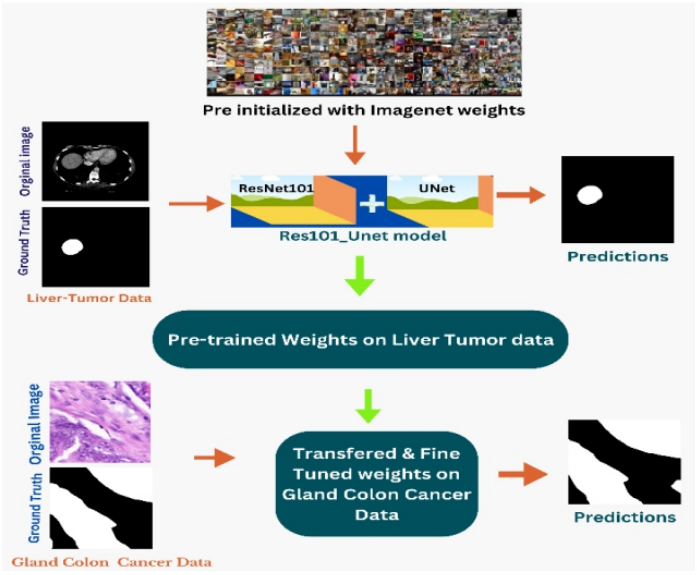

Fig. 2: Process Flow of The Proposed Transfer Learning Methodology

ResNet101 model Description: ResNet-101 is a convolutional neural network (CNN) architecture from the ResNet (Residual Network) family. ResNet-101 is made up of 101 layers, making it deeper than previous versions like ResNet-18, ResNet-34 and ResNet-50 [11]. ResNet models, particularly ResNet-

101, are distinguished by their usage of residual connections, also known as skip connections or shortcut connections. These connections let input to travel through one or more layers, allowing the model to learn residual mappings rather than the desired underlying mapping. This helps to mitigate the vanishing gradient problem and makes it easier to train very deep neural networks. ResNet-101 is frequently used for a variety of computer vision applications, such as image classification, object recognition, and segmentation. It has attained cutting-edge performance on a number of benchmark datasets and is widely regarded as one of the most powerful and effective CNN designs.

U-Net model Description: Convolutional neural network architecture U-Net was created specifically for biomedical image segmentation. It is composed of two paths: an expanding path that enables precise localization through up sampling and convolutional layers, and a contracting path that gathers context through convolutional and pooling layers. U-Net's symmetric construction makes it possible to train it efficiently on small datasets, which makes it useful for a variety of applications like organ and cell segmentation, lesion detection, satellite image analysis, and industrial inspection.

The following figure displays the model architecture of Res101_Unet.

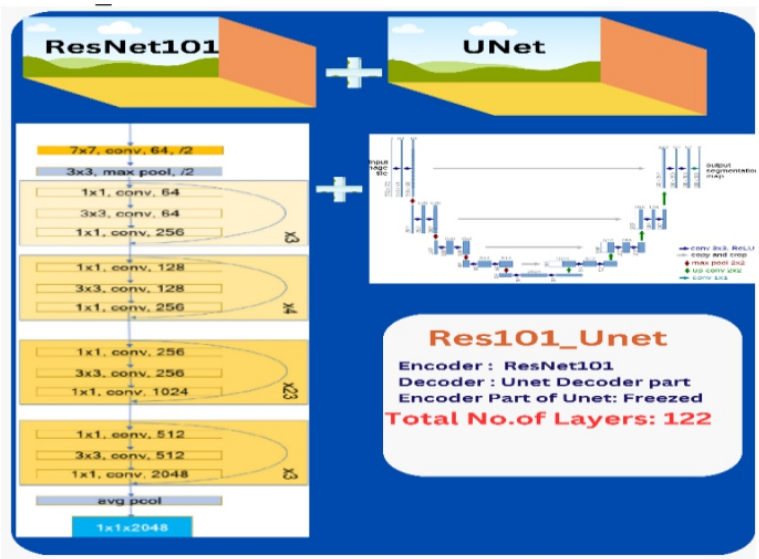

Fig. 3: Architecture of Res101_Unet

Res101_Unet description: A hybrid convolutional neural network architecture called ResNet101-Unet combines the precise segmentation capabilities of the U-Net architecture with the feature extraction capabilities of the ResNet-101 backbone. The vanishing gradient issue is solved by residual connections, and feature maps are up-sampled for a segmentation mask with the same spatial resolution as the input image using a U-Net decoder.

IV. DATASET AND PREPROCESSING

The 3DIRCADB-Liver tumor dataset and the GlaS@MICCAI'2015: Gland Segmentation-Gland-colon cancer dataset, which are both publicly available benchmark medical imaging datasets, were obtained via the Kaggle data science competition hosting portal [8][9][10]. The 2D samples in the collection are included, together with binary masks that isolate the tumor and leave the surrounding area as background. The dataset's attributes are listed in the following table.1.

Table. 2: Overview of the Data

Dataset	Attributes		
	Image Size	Mode	No. of Samples
Liver Tumor	512*512	Grayscale	2058
Gland Colon Cancer	775*522	RGB	85

The following figure shows the sample instances of the datasets used in this study.

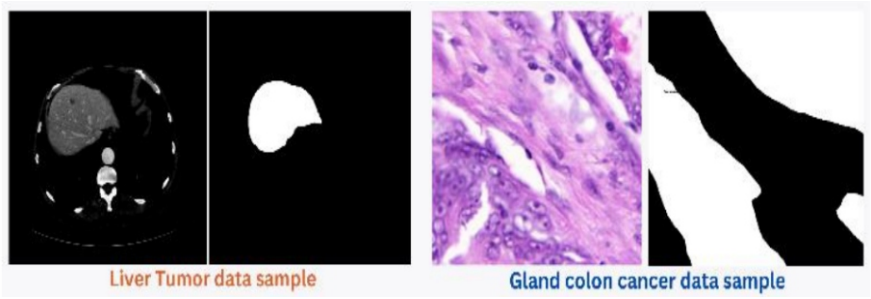

Fig. 4. Dataset Sample Instances and Masks of Liver and Gland Colon Tumors

It is clear that in transfer learning, the knowledge gained during training with a moderately large dataset can be applied to segment the data scared areas, such as gland colon segmentation, where we have very few samples (85), limiting us to do standalone training with the data because deep learning expects more data to perform better. However, our study demonstrates that the application of domain similarity based transfer learning leverages good results and optimal performance with less data because both the pre-trained dataset and the target dataset belong to the medical imaging domain, and the targets are tumor parts that are mostly similar in shape and texture.

The figure below depicts the dataset folder structure and preparation methods utilized in the experimental study, along with a thorough description of the steps.

Dataset	Data set split ratios (0.7 ,02, & 0.1)			
	Total No. of samples	*Training*	*Validation*	*Testing*
Liver-Tumor	2058	1440	464	154
Gland-Colon-Cancer	85	60	18	7

Dataset	*Details of Pre processing*			
	Scaling	Normalization	Denoising Filter	Data Augmentation
Liver Tumor	256*256*3	Yes	Bilateral Gaussian	No
Gland Colon Cancer	256*256*3	Yes	Bilateral Gaussian	Yes

Fig. 5: Overview of Dataset Organization, Splitting, and Preprocessing

The Resnet is pre-trained on the ImageNet dataset, which contains color images with dimensions of 256*256. Initially, all images are resized to 256*256 and pixel-wise normalized by dividing each pixel by 255. Both datasets are preprocessed with a Bilateral Gaussian noise filter to perform denoising and improve the clarity of low contrasted medical images, followed by histogram equalization. Data augmentation is only used to the gland colon dataset to enhance the number of samples. The built-in augmentation attributes and standard processes available in the Keras API are used to enrich the data.

V. EXPERMENTAL SETUP

In this study, a Kaggle Notebook with G100 GPU processor and Google Colab's T4 GPU were used as the experimental setup for training, evaluating, and inferring on Res101_Unet. Strong computational resources are required for effective deep learning model training, which is what drove this decision. For quick experimentation, the open-source segmentation models API was used to explore different model structures and setups. To extract features from the liver data, the U-Net model was first trained using various backbone architectures, particularly ResNet. Testing of the ResNet-34 and ResNet-50 backbones yielded results that fell short of the intended performance requirements. As a result, research was conducted on the ResNet-101 backbone, a deep layer neural network with 99 convolutional layers that is regarded as a cutting-edge model for computer vision applications. with a Intersection over Union (IoU) of 0.9891and training and testing accuracies of 98.25% and 97.60%, respectively, throughout 100 training epochs, this model proved to be exceptionally effective.

Plots were used to show the comparative performance of the ResNet-34 U-Net, ResNet-50 U-Net, and ResNet-101 U-Net models, allowing for a clear grasp of the models' effectiveness. The training parameters were the Adam optimizer, the Binary Cross-Entropy loss function, a learning rate of 0.0001 (1e-4), and 100 epochs.

Following the successful training of the ResNet-101 U-Net model on liver tumor data, the pre-trained weights were used to fine-tune the model on Gland colon cancer dataset. This transfer learning technique produced promising findings, demonstrating its potential use in comparable research situations. The experimental findings section contains a detailed analysis of the results, emphasizing the efficiency of the model and training settings.

The code and implementation can be downloaded from the following: https://github.com/rddvsr/ABMIS-DCNN.git

VI. RESULTS AND DISCUSSION

This section presents and analyzes the qualitative and quantitative findings from our experimental study. Figure.6compares the qualitative results of Res101_Unet to those of swallow Res_Unets, while Table.3 summarizes the quantitative metrics used to analyze the model's performance. The training, validation, and testing accuracies along with the IoU Score are shown it clearly demonstrate the proposed model's performance.

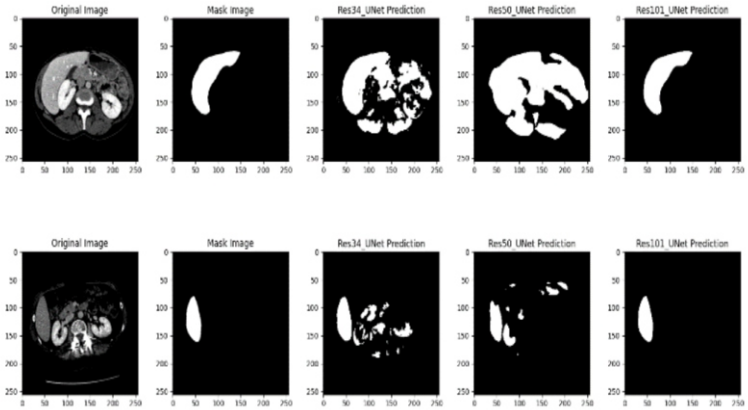

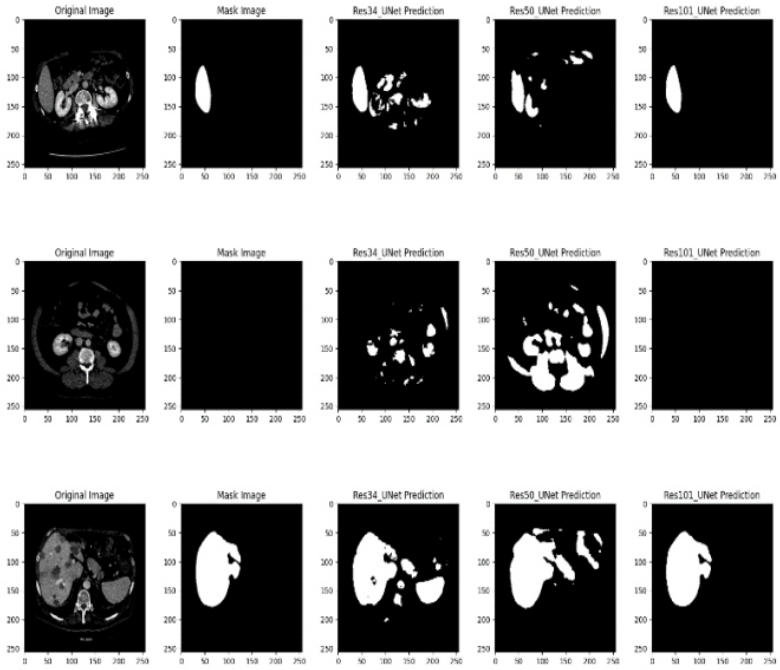

Fig. 6: Comparative Qualitative Predictions of ResNet-101 U-Net and Swallow Res_Unets.

Table. 3: Quantitative results of the Res101_Unet

Data → / Metrics ↓	Liver Tumor data			Gland Colon data		
	Train	Val	Test	Train	Val	Test
Accuracy	0.9825	0.9829	0.9760	0.6956	0.6559	0.6816
Loss	0.0037	0.0048	0.0098	0.2240	0.4719	0.2880
IoU Score	0.9891	0.9821	0.9724	0.7043	0.6558	0.6780

We have conducted several training trails by changing the various hyper parameters for training on the gland colon dataset. We have achieved best results as shown in the Table.3 by applying cross-fold validation with limited data augmentation. The following Table.4 shows the hyper parameters used for the training and fine tuning.

Table. 4: Details of the Hyper Parameters used in the Experimental Study

Data → / Hyper Parameters ↓	Liver Tumor Data	Gland Colon Data
No.of Epochs	100	100
Loss function	Binary_Crossentropy	Binary_Crossentropy
Optimizer	Adam	Adam
Learning Rate	0.00001	0.001
Data Augmentation	No	Yes
Cross-fold verification	No	Yes 5-fold cross validation used

Some of the predictions of Res101_Unet on sample test data is shown below further finetuning can be done to get the better accuracy.

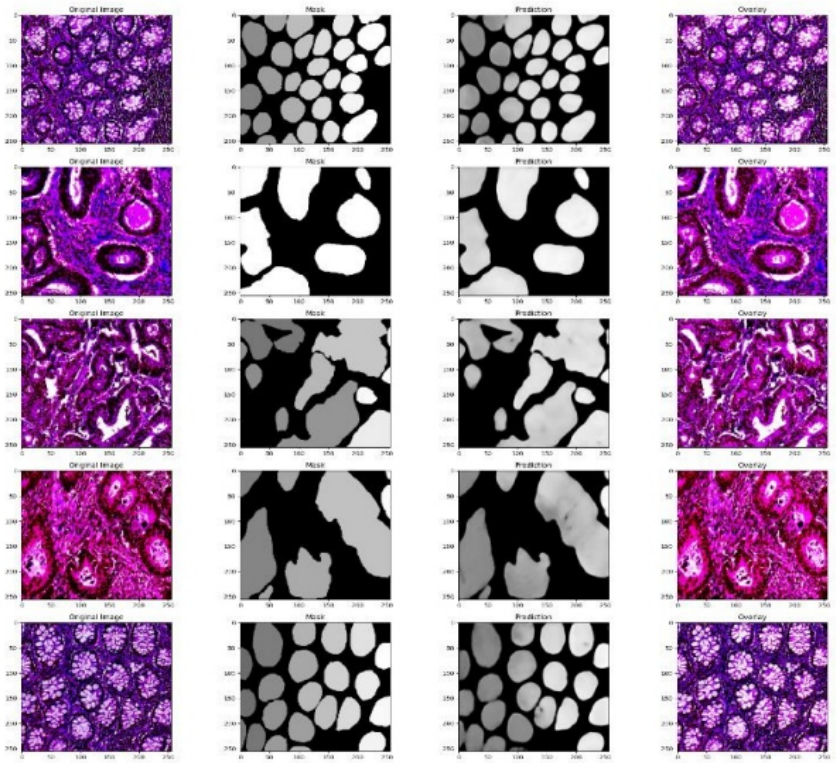

Fig. 7: Comparative Qualitative Predictions of ResNet-101 U-Net on Gland Colon Test Data

VII. CONCLUSION

This work describes a parameter-based transfer learning strategy for medical image segmentation. Our results show that the Res101_Unet model can achieve accurate image segmentation even with limited data availability. Using deep-layer networks allows to extract fine-grained information from the source domain and apply it efficiently to target domains. This capability proves particularly valuable for segmenting tumor sections characterized by diverse forms and sizes. As an extension of this, generic tumor segmentation models can be trained on Res101_Unet using mixed tumor datasets from other organs.

ACKNOWLEDGMENT

We are grateful to the Visvesvaraya Ph.D. scheme, Digital India Corporation, MHRD, India for supporting research through funding.

DECLARATION STATEMENT

Funding	No funding received.
Conflicts of Interest	No conflicts of interest to the best of our knowledge.
Ethical Approval and Consent to Participate	No, the article does not require ethical approval and consent to participate with evidence.
Availability of Data and Material/ Data Access Statement	Not relevant.
Authors Contributions	All authors have equal participation in this article.

REFERENCES

1. Zhang, Jing & Li, Wanqing & Ogunbona, Philip. (2017). https://www.researchgate.net/publication/316921517_Transfer_Learn ing_for_Cross-Dataset_Recognition_A_Survey

2. Ronneberger O., Fischer P., Brox T. (2015) U-Net: Convolutional Networks for Biomedical Image Segmentation. In: Navab N., Hornegger J., Wells W., Frangi A. (eds) Medical Image Computing and Computer-Assisted Intervention – MICCAI 2015. MICCAI 2015. Lecture Notes in Computer Science, vol 9351. Springer, Cham. https://doi.org/10.1007/978-3-319-24574-4_28.https://doi.org/10.1007/978-3-319-24574-4_28

3. Badrinarayanan, Vijay et al. "SegNet: A Deep Convolutional Encoder-Decoder Architecture for Image Segmentation." IEEE Transactions on Pattern Analysis and Machine Intelligence 39 (2017): 2481-2495. https://doi.org/10.1109/TPAMI.2016.2644615

4. Chen, Liang & Bentley, Paul & Mori, Kensaku & Misawa, Kazunari & Fujiwara, Michitaka & Rueckert, Daniel. (2018). DRINet for Medical Image Segmentation. IEEE Transactions on Medical Imaging. PP. 1-1. 10.1109/TMI.2018.2835303.https://doi.org/10.1109/TMI.2018.2835303

5. Krupinski, Elizabeth. (2016). Medical Imaging. 10.1007/978-3-319-14346-0_186. https://www.researchgate.net/publication/310238383_Medical_Imaging. https://doi.org/10.1117/1.JMI.3.1.011001

6. J. Deng, W. Dong, R. Socher, L. -J. Li, Kai Li and Li Fei-Fei, "ImageNet: A large-scale hierarchical image database," 2009 IEEE Conference on Computer Vision and Pattern Recognition, 2009, pp. 248-255, doi: 10.1109/CVPR.2009.5206848.https://doi.org/10.1109/CVPR.2009.5206848

7. Raghu, M., Zhang, C., Kleinberg, J.M., & Bengio, S. (2019). Transfusion: Understanding Transfer Learning for Medical Imaging. NeurIPS.

8. Kaggle Competitions. (n.d.). https://www.kaggle.com/competitions

9. 3DIRCADB. (2022, February 19). Kaggle. https://www.kaggle.com/datasets/nguyenhoainam27/3dircadb

10. GlaS@MICCAI'2015: Gland Segmentation. (2022, June 6). Kaggle. https://www.kaggle.com/datasets/sani84/glasmiccai2015-gland-segmentation

11. K. He, X. Zhang, S. Ren and J. Sun, "Deep Residual Learning for Image Recognition," 2016 IEEE Conference on Computer Vision and Pattern Recognition (CVPR), Las Vegas, NV, USA, 2016, pp. 770-778, doi: 10.1109/CVPR.2016.90.https://doi.org/10.1109/CVPR.2016.90

12. Huang, H., Chen, H., Xu, H. et al. Cross-Tissue/Organ Transfer Learning for the Segmentation of Ultrasound Images Using Deep Residual U-Net. J. Med. Biol. Eng. 41, 137–145 (2021). https://doi.org/10.1007/s40846-020-00585-w

13. Huang, Z., Wang, H., Deng, Z., Ye, J., Su, Y., Sun, H., ... & Qiao, Y. (2023). Stu-net: Scalable and transferable medical image segmentation models empowered by large-scale supervised pre-training. arXiv preprint arXiv:2304.06716.

14. Hosseinzadeh Taher MR, Haghighi F, Feng R, Gotway MB, Liang J. A Systematic Benchmarking Analysis of Transfer Learning for Medical Image Analysis. Domain Adapt Represent Transf Afford Healthc AI Resour Divers Glob Health (2021). 2021 Sep-Oct;12968:3-13. doi: 10.1007/978-3-030-87722-4_1. Epub 2021 Sep 21. PMID: 35713581; PMCID: PMC9197759. https://doi.org/10.1007/978-3-030-87722-4_1

15. Nampalle, Kishore Babu & Uppala, Vivek & Raman, Balasubramanian. (2023). Transfer learning-based framework for image segmentation using medical images and Tversky similarity. 10.21203/rs.3.rs-2587704/v1.https://doi.org/10.21203/rs.3.rs-2587704/v1

16. Karimi D, Warfield SK, Gholipour A. Transfer learning in medical image segmentation: New

insights from analysis of the dynamics of model parameters and learned representations. Artif Intell Med. 2021 Jun;116:102078. doi: 10.1016/j.artmed.2021.102078. Epub 2021 Apr 23. PMID: 34020754; PMCID: PMC8164174.https://doi.org/10.1016/j.artmed.2021.102078

17. Ghavami, A. (2023). Image segmentation using UNet architecture in Pytorch for biomedical image processing. Retrieved from arXiv preprint arXiv:2305.14841v1.

18. Poudel, K., Dhakal, M., Bhandari, P., Adhikari, R., Thapaliya, S., & Khanal, B. (2023). Exploring Transfer Learning in Medical Image Segmentation using Vision-Language Models. ArXiv, abs/2308.07706.

19. Papers with Code - Transfer Learning U-Net Deep Learning for Lung Ultrasound Segmentation. (2021, October 5). https://paperswithcode.com/paper/transfer-learning-u-net-deep-learning-for

20. Das, S., S, S., M, A., & Jayaram, S. (2021). Deep Learning Convolutional Neural Network for Defect Identification and Classification in Woven Fabric. In Indian Journal of Artificial Intelligence and Neural Networking (Vol. 1, Issue 2, pp. 9–13). https://doi.org/10.54105/ijainn.b1011.041221

21. Kanani, P., & Padole, Dr. M. (2019). Deep Learning to Detect Skin Cancer using Google Colab. In International Journal of Engineering and Advanced Technology (Vol. 8, Issue 6, pp. 2176–2183). https://doi.org/10.35940/ijeat.f8587.088619

22. Wanjau, S. K., Wambugu, G. M., & Oirere, A. M. (2022). Network Intrusion Detection Systems: A Systematic Literature Review of Hybrid Deep Learning Approaches. In International Journal of Emerging Science and Engineering (Vol. 10, Issue 7, pp. 1–16). https://doi.org/10.35940/ijese.f2530.0610722

23. Behera, D. K., Das, M., & Swetanisha, S. (2019). A Research on Collaborative Filtering Based Movie Recommendations: From Neighborhood to Deep Learning Based System. In International Journal of Recent Technology and Engineering (IJRTE) (Vol. 8, Issue 4, pp. 10809–10814). https://doi.org/10.35940/ijrte.d4362.118419

24. Nikam, S. S., & Dalvi, Prof. R. (2020). Fake News Detection on Social Media using Machine Learning Techniques. In International Journal of Innovative Technology and Exploring Engineering (Vol. 9, Issue 7, pp. 940–943). https://doi.org/10.35940/ijitee.g5428.059720

AUTHORS PROFILE

D D V Sivaram Rolangi, Research Scholar, Department of Computer Science and Systems Engineering, Andhra University college of Engineering, Andhra University, completed his B. Tech in Computer Science and Engineering from V R Siddhartha Engineering College, Vijayawada, India. M.Tech in Information Technology and pursuing his Ph.D from Andhra University College of Engineering , Andhra University, Visakhapatnam, India. His areas of interests include Theoretical Computer Science, Compiler technologies, Network programming. He has about 18 years of experience in teaching. His research interests include Machine learning, Computer vision, Deep learning, IoT and Assistive Technologies. He is currently working as Assistant Professor in Department of Computer Science and Engineering, University College of Engineering Vizianagaram-JNTU-GV, Vizianagaram, India.

Lalitha Bhaskari D, Professor, Department of Computer Science and Systems Engineering, Andhra University college of Engineering, Andhra University, Visakhapatnam, India, pursued her Bachelor of technology and Master of Technology from Andhra University Visakhapatnam, India in the year 1997 and 2001 respectively. She completed her Ph.D. from JNTU, Hyderabad in the year 2009. She is currently working as Professor in the Department of Computer Science and Systems Engineering, Andhra University with 26 years of teaching experience. She has authored over 60 scientific research articles in referred international journals and conferences. Her professional services include - but not limited to - Industry consultations, a workshops chair, a technical program committee member, and a reviewer for several many reputed international conferences and journals. Her main research work focuses on Cryptography & Network Security, Stenography & Digital Watermarking, Pattern Recognition, Image Processing, Computer vision, Cyber Crime & Digital Forensics.

SUPPLEMENTARY DATA

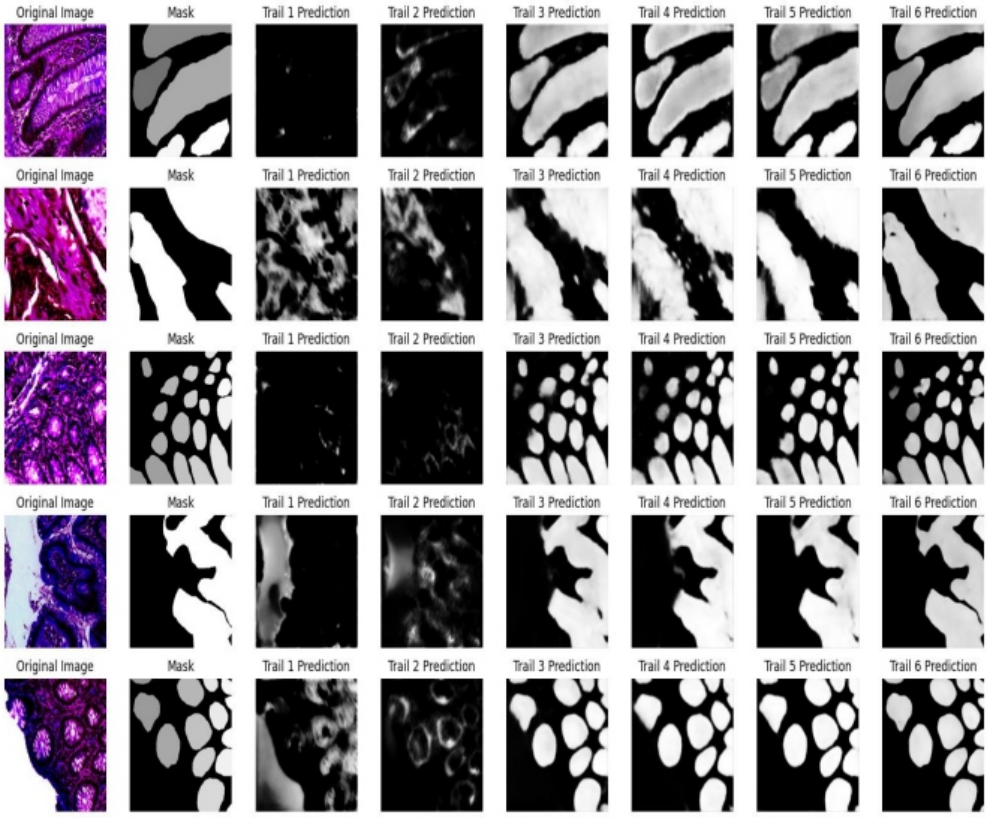

Fig. 8: Comparative Trails Qualitative Predictions of ResNet-101 U-Net on Gland Colon Test data

ISSN: 2249-8958

Domestic Cats Facial Expression Recognition Based on Convolutional Neural Networks

Abubakar Ali, Crista Lucia Nchama Onana Oyana, Othman S. Salum

A B S T R A C T

Despite extensive research on Facial Expression Recognition (FER) in humans using deep learning technology, significantly less focus has been placed on applying these advancements to recognize facial expressions in domestic animals. Recognizing this gap, our research aims to extend FER techniques specifically to domestic cats, one of the most popular domestic pets. In this paper, we present a real-time system model that employs deep learning to identify and classify cat facial expressions into four categories: Pleased, Angry, Alarmed, and Calm. This innovative model not only helps cat owners understand their pets' behavior more accurately but also holds substantial potential for applications in domestic animal health services. By identifying and interpreting the emotional states of cats, we can address a critical need for improved communication between humans and their pets, fostering better care and well-being for these animals. To develop this system, we conducted extensive experiments and training using a diverse dataset of cat images annotated with corresponding facial expressions. Our approach involved using convolutional neural networks (CNNs) to analyze and learn from the subtleties in feline facial features by investigating the models' robustness considering metrics such as accuracy, precision, recall, confusion matrix, and f1-score. The experimental results demonstrate the high recognition accuracy and practicality of our model, underscoring its effectiveness. This research aims to empower pet owners, veterinarians, and researchers with advanced tools and insights, ensuring the well-being and happiness of domestic cats. Ultimately, our work highlights the potential of FER technology to significantly enhance the quality of life for cats by enabling better understanding and more responsive care from their human companions.

Keywords: Facial Expression Recognition, Domestic Cats, CNN, Haar Cascade Classifier, Deep learning.

I. INTRODUCTION

In recent years, interest has surged in using machine learning techniques, especially Convolutional Neural Networks (CNNs), for human facial expression recognition [1][33][34]35]. The findings from these studies show great promise in accurately identifying and categorizing facial expressions, opening up new possibilities for applications in veterinary science and animal behavior research. However, the majority of these studies have focused on species other than domestic cats, leaving a notable gap in the literature regarding automated facial expression recognition specifically tailored to felines [2]. Domestic cats, beloved companions to millions of people worldwide, possess a rich array of facial expressions that communicate various emotions and states of being (L. Dawson et al.) [3]. Understanding these expressions is not only fascinating from a behavioral standpoint but also crucial for enhancing the human-feline bond and potentially improving veterinary care. However, accurately interpreting feline facial expressions poses a significant challenge due to the subtle nuances and complexities involved [4].

Moreover, Despite the acknowledged importance of understanding feline facial expressions, the area of automated recognition and interpretation of these expressions is still largely uncharted [5]. Traditional methods for studying facial expressions in cats rely heavily on subjective human interpretation, which

can be inconsistent and prone to biases. Additionally, the lack of standardized facial expression databases for cats further complicates the development of accurate recognition systems. One significant area requiring improvement in the field of domestic cat facial expression recognition is the development of robust CNN models trained on annotated datasets of feline facial expressions. Existing datasets for other species, such as humans and dogs, may not adequately capture the diverse range of facial expressions exhibited by cats [6]. Furthermore, Standardized protocols for capturing and annotating facial expressions are necessary to ensure consistency and reliability in training and evaluating CNN models. Overcoming these challenges is crucial for advancing the automated recognition of domestic cat facial expressions and realizing its full potential in various practical applications. This paper seeks to advance the growing body of research in this area by presenting a method for recognizing domestic cat facial expressions using Convolutional Neural Networks. We will detail the methodology for collecting and annotating a dataset of feline facial expressions, along with the implementation of the CNN model on our customized domestic cat dataset.Additionally, we will present experimental results demonstrating the effectiveness of our approach and discuss potential applications and future directions for research in this exciting area. So, our contributions to this paper are asfollows:

- This study intends to contribute insights into the effectiveness of Recognizing Facial Expressions of Domestic Cats.
- Develop a Customized dataset of domestic Cats' facial expressions representing four emotional states which are angry, calm, pleased, and alarmed.
- Evaluate the performance of the proposed model and assess its potential applications in the facial expression recognition of domestic cats considering metrics such as accuracy, recall, precision, f1-score, Bar chart, and confusion matrices.
- Additionally, this research aims to highlight potential areas for improvement and future directions in the development of emotion detection in domestic animals and potential applications in animal welfare, behavior analysis, and human-animal interaction.

II. RELATED WORK

Lin and Kuo et al. [7] focus on individual cat identification. They train a CNN to detect the facial features of cats but for identification, they use conventional machine learning methods (SVMs and PCA). A tiny data set of 150 cats' 1,500 images is also used by them. From the publication, it is unclear whether the 94.1% claimed identification accuracy includes or excludes people or training images.

L. Xingxing et al. [8] offered an experimental evaluation of the system model's only on Cat face detection. They applied a Haar rectangular eigenvalue-integral graph and extractedfeatures of a cat face. Then screened features for classification and recognition. Nevertheless, they applied the AdaBoost to alter a feeble classifier into a robust classifier that can effectually recognize cat faces. The use of the Gaussian Mixture Model with Mel-Frequency Cepstrum Coefficients for cat face recognition is highlighted by (Yu Fan and Chen et al., 2021) [9].

They used these approaches to identify the distinctive characteristics of cats and were utilized as an innovation to extract cat facial features after the Gaussian Mixture Model was created for each cat. For assessing the model's parameters, the maximum likelihood estimate is utilized. Although there are just 30 Cat faces in the dataset used for their study. An approach for cat recognition and identification that uses autoencoders combined with convolutional neural networks (CNN) was proposed by (P.Chen et al.,2021) [10].

They also produced a brand-new dataset with 1,994 images of 17 cats. Additionally, they provided a thorough explanation of how to use Autoencoder to denoise cat image data and combine it with CNN to

produce a powerful model for the same cat recognition for future study.

III. METHODS

The proposed system models consist of a Convolutional Neural Network (CNN) by classifying domestic cat facial expression recognition. Figure 1 below, summarize the process of classifying the cat's emotions from the input image. It comprises the following steps, image processing, feature extraction, and classification. all of the steps are very significant for analyzing models for Cat facial expression recognition.

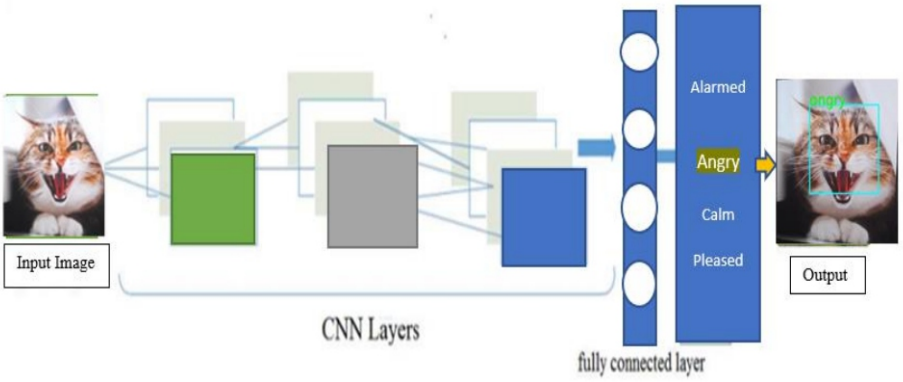

Figure 1. The Process Diagram Representation of Classifying Domestic Cats' Facial Expression Recognition

A.Dataset Preparation

In this study, we collected the domestic cats faces images with an input of a resolution of 64x64. The Dataset is a meticulously organized collection of cat facial expressions, categorized into four distinct emotional states: 'calm', 'alarmed', 'angry', and 'pleased' as illustrated by Figure 2 below. This dataset serves as a valuable resource for researchers and developers interested in exploring the nuances of feline emotional expression and behavior. Each image in the dataset captures the unique facial features and expressions exhibited by domestic cats in various contexts.

In addition, before training the deep learning model, the dataset undergoes several pre-processing steps to enhance model performance and facilitate efficient training [11]. These pre-processing steps ensure robust model training the steps are as follow. Image resizing: Resizing images to a uniform resolution to ensure consistency and reduce computational complexity during training, in this study, we resize the images to 64 x 64. Data augmentation: we applied various augmentation techniques such as rotation, flipping, cropping, and brightness adjustment to increase the diversity and size of the dataset, thereby improving model generalization. Flip: Horizontal, Vertical, Crop: 0% Minimum Zoom, 20% Maximum Zoom, Rotation: Between -15° and +15°, Grayscale: Apply to 15% of images, Brightness: Between -15% and +15%, and Noise: Up to 0.1% of pixels . Furthermore, as part of the preprocessing pipeline, all images in the dataset have undergone normalization to enhance model convergence and performance. Normalization ensures that the input data is standardized, reducing the impact of variations in pixel intensity and improving the overall stability of the training process [12]. Moreover, a Domestic cats customized dataset of a total of experimental numbers for each expression is shown in Table 1 below.

Figure 2. Illustration of the Proposed Facial Expression Distribution, the Pictures Convey A Variety of Feelings

Table 1. The Experimental Number of Customized cat Dataset

Expression Label	Cat dataset
Alarmed	199
Angry	200
Calm	200
Pleased	200

B.Proposed Model Architecture

Our proposed model's structure is a pure convolutional network. The architecture of the model employed in our project is shown in Figure 3 below.

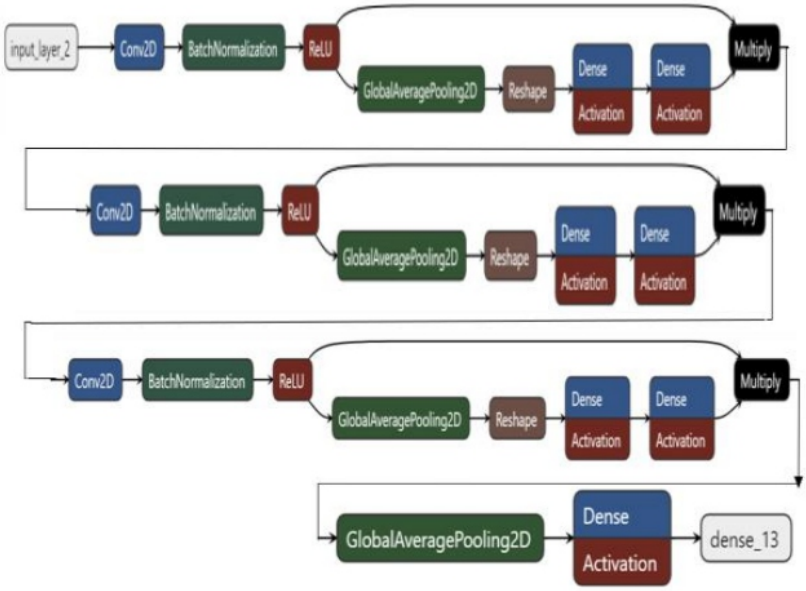

Figure 3. The Proposed Model Architecture is a Series of Convolutional Layers Connected with the Squeeze-and-Excitation Block, Leading to a SoftMax Classifier that Outputs the Probability Value

The first layer of the Proposed model architecture is the Convolution Layer [13], it extracts the significant features from the input image which is denoted as pixel values in the form of a matrix. In the convolution operation, the filter is the first part involved and the stride parameter controls how the filter moves across the image. In addition, the filter goes over the image one pixel at a time when the step is 1, and two pixels at a time when the step is 2 [14]. Additionally, the convolution process is calculated by multiplying the two matrices, where the first matrix is the input image and the second matrix is the filter

matrix is the input image and the second matrix is the filter or kernel (Zeiler & Fergus, 2014)[15]. The input image is the result of adding each element of the input image to its neighbor's weights. Moreover, the activation/feature map is the name of the convolution operation's output. Mathematically, the convolution operation for a 2D input can be expressed as:

$$(I * K)(i,j) = \sum_m \sum_n I(i+m, j+n) \cdot K(m,n) \quad (1)$$

Here, ***I*** is the input data. **K** is the convolutional filter (kernel). (i, j) represents the position in the output feature map.(m, n) iterates over the filter dimensions.

Furthermore, the output of the convolution process is known as the activation or feature map and the most frequently practical activation function is the ReLU layer (Rectified Linear Unit) which is applied to nonlinearity into the output(Krizhevsky et al., 2017) [16]. The ReLU function returns to 0 if all of the input values are negative, and to (x) if all of the input values are positive. The result is a rectified feature map. The ReLU activation function is provided by equation (2)Moreover, the Spatial pooling layer is applied to diminish the number of parameters in a big image and it is also known as up-sampling and down-sampling. Nevertheless, the purpose of this layer is to reduce the size of the feature map while maintaining the important portions of the image (S. Lawrence et al., 1997) [17]. There are three (3) main types of spatial pooling, the first type is max pooling which is used to take the biggest component of the corrected activation map.The mathematical formula for Max Pooling can be defined as follows:

$$\text{Max Poling}(x,s)_{i,j} = \max_{m,n} \left(x_{i \cdot s+m, j \cdot s+n}\right) \quad (3)$$

Here: **x** is the input volume. s is the stride of the pooling operation, representing the step size with which the pooling window moves. **i** and **j** are the indices of the output feature map.**m** and **n** iterate over the spatial dimensions of the pooling window. In simpler terms, for each position (i, j) in the output feature map, the Max Pooling operation looks at the region in the input volume defined by the size of the pooling window and the stride. It then selects the maximum value from that region

The second type is average pooling (Szegedy et al., 2015)[18], which is practical for selecting the average values of the element in the rectified feature map. The third type is Sum pooling which is used to sum all available elements in the rectified feature map. Additionally, a crucial technique for lowering the measurement after the convolution layer is this layer. Average Pooling is another commonly used pooling operation, and it calculates the average value of the elements in the pooling window. The formula for Average Pooling is:

$$\text{Average Pooling}\ (x,s)_{i,j} = \frac{1}{m \cdot n} \sum_{m,n} \left(x_{i \cdot s+m, j \cdot s+n}\right) \quad (4)$$

Here, the average is taken over all the elements in the pooling window. In both cases, the pooling operation helps reduce the spatial dimensions of the input volume, making it computationally more efficient while retaining important features. The choice between Max Pooling and Average Pooling often depends on the specific requirements of the task and the characteristics of the data.

Also, Convolution layer expansion can exacerbate the issue of a generic pooling technique that explores feature maps (M. Jogin et al.,2018) [19]. In addition to the above, after completing the technique of spatial pooling. After the 2-dimensional matrix is flattened into a linear-continuous long vector in the following layer, it is passed to a fully connected layer for classification.

Finally, fully connected layer denotes every neuron being linked to every other neuron. This completely linked layer receives the output from the flattened layer, which transforms the two-dimensional matrix

into a long vector (S. Lawrence et al., 1997) [20]. After training, the feature vector from this layer is subsequently used to divide images into distinct classes. Moreover, in this layer, all the inputs are linked to every activation part of the next layer. Since all the parameters are occupied in the fully connected layer, it causes overfitting. So, dropout is one of the methods that diminishes overfitting.

After passing through the stage of this layer, the SoftMax activation function is the final layer which is applied to obtain the object's probability based on input that falls into particular classes (S. Shalev-Shwartz et al.) [21].

C.Implementation and Training Model Parameters

a. Implementation

We innovated our model by adding The Squeeze-and-Excitation (SE) block. it is a novel architectural unit designed to improve the representational power of convolutional neural networks by enabling them to perform dynamic channel-wise feature recalibration. Introduced by (Jie Hu, and Gang Sun, 2018) [22], in their paper "Squeeze-and-Excitation Networks," the SE block aims to enhance the quality of the feature maps generated by a CNN.Figure 4 provides an illustration of the fundamental structure of the SE block.

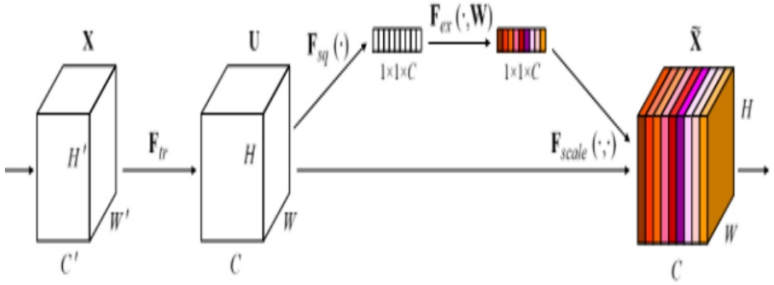

Figure 4. Squeeze-and-Excitation (SE) Block [22]

The core idea is to explicitly model the interdependencies between the channels of the convolutional features. This process involves two main operations: squeeze and excitation. In the "squeeze" step, global average pooling is applied to each feature map independently, producing a channel descriptor that captures global spatial information. This step reduces each 2D feature map into a single numerical value, summarizing the entire spatial extent. Following this, the "excitation" step consists of two fully connected (dense) layers that form a self-gating mechanism. The first dense layer reduces the number of channels by a reduction ratio (typically set to 16), capturing the channel interdependencies with a non-linear transformation. The second dense layer restores the original number of channels. The output of this second layer is passed through a sigmoid activation function to generate a set of weights between 0 and 1. These weights act as adaptive recalibration parameters that scale the original feature maps channel-wise [22]. Byemphasizing important features and diminishing less useful ones, the SE block allows the network to focus more on informative features, thereby improving the overall performance. The entire SE block operation can be summarized as:

$$\mathbf{X'}_{i,j,c}=\mathbf{X}_{i,j,c}\cdot\sigma 2(\mathbf{W}2\sigma 1(\mathbf{W}1\mathbf{z}))c \qquad (5)$$

where **z** is the squeezed vector obtained from global average pooling, **W**1 and **W**2 are the weight matrices of the two fully connected layers, and σ1 and σ2 are the ReLU and sigmoid activation functions, respectively. The equation 5 describes how the SE block adaptively recalibrates the channel-wise

feature responses by leveraging global information, thus enhancing the representational capacity of the network.

b. Training Model Parameters

The model parameters in the context of neural networks refer to the settings that define the architecture and behavior of the network, such as learning rate, batch size, optimizer,etc. [23]. The following hyperparameters were applied. a learning rate of 0.001 was used during training. Correspondingly, the batch size of 64 was applied, Batch size refers to the number of samples processed in one forward and backward pass during training. Also, the Categorical Cross-Entropy Loss Function was applied during training. It measures the dissimilarity between the predicted probability distribution and the true distribution of class labels [24]. In addition, for the model optimization, The Adam optimizer was applied in this study, it combines the benefits of both momentum and RMSprop optimization techniques. The algorithm is known for its efficiency, fast convergence, and robustness to different types of data [25]. Table 2. Displaythe experimental parameters applied in this study on Customized Cats datasets.

Table 2. Experimental Model Parameters on Cats Dataset

Learning Rate	Batch Size	Optimizer	Image Size
0.001	64	Adam	64x64

IV. RESULT AND DISCUSSION

A.Result

The Experimental Result of the proposed model fordomestic cats' facial expression recognition was evaluated using a set of evaluation metrics, including precision, recall, F1 score, training accuracy, training loss, and a confusion matrix. We can observe that the model achieved good results in the different facial expressions. As can be observed from Table 3 which reveals the performance metrics results values in all four domestic cats' facial expressions with their support values.

Table 3. The Proposed Model Evaluation Results on Domestic Cats Dataset

Metrics / Cats Data	Precision	Recall	F1-Score	Support
Alarmed	0.99	0.95	0.97	199
Angry	0.98	0.99	0.99	200
Calm	0.97	0.98	0.97	200
Pleased	0.99	0.99	0.99	200
Accuracy			0.98	799
Macro avg	0.98	0.98	0.98	799
Weighted avg	0.98	0.98	0.98	799

Precision metric measures the proportion of correctly predicted positive cases out of all cases predicted as positive as expressed in equation 1 below [26].

$$\text{Precision} = \frac{\text{True Positives}}{\text{True Positives} + \text{False Positives}} \quad (1)$$

For the Alarmed expression, the precision is very high at 0.99, indicating that when the model predicts an

Similarly, for Angry and Pleased expressions, the precision values are also high, at 0.98 and 0.99 respectively, indicating high accuracy in identifying these expressions. Moreover, the recall metric measures the proportion of correctly predicted positive cases out of all actual positive cases which is expressed in Equation 2 [27].

$$\text{Recall} = \frac{\text{True Positives}}{\text{True Positives} + \text{False Negatives}} \quad (2)$$

For the Alarmed expression, the recall is 0.95, implying that the model correctly identifies 95% of all actual Alarmed instances. For Angry, Calm, and Pleased expressions, the recall values are notably higher, indicating that the model performs very well in capturing instances of these expressions. Furthermore, the f1-score is the harmonic mean of precision and recall, providing a balanced measure that considers both false positives and false negatives as given in equation 3 below [28].

$$f1 - score = \frac{2 \times \text{Precision} \times \text{Recall}}{\text{Precision} + \text{Recall}} \quad (3)$$

Across all classes, the f1-scores are consistently high, ranging from 0.97 to 0.99, indicating overall strong performance of the model in terms of both precision and recall. Lastly, the accuracy metric measures the overall correctness of the model's predictions across all classes. With an accuracy of 0.98, it indicates that the model correctly predicts the facial expressions in the customized dataset with a high degree of accuracy.

The training accuracy and loss graphs illustrate the learning progression over epochs. They show how the accuracy of the model improves and the loss decreases as the training proceeds. Figure 5 reveals the training loss and accuracy of the proposed model in the customized domestic cats' dataset, the suggested model's validation accuracy is shown alongside its training accuracy.

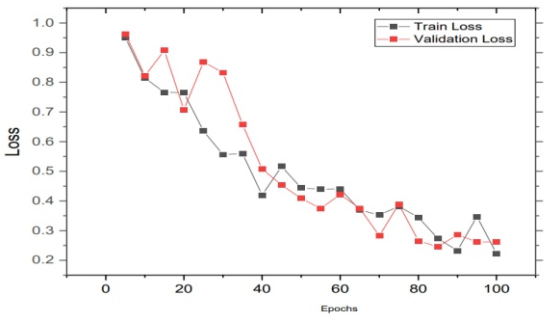

(a)

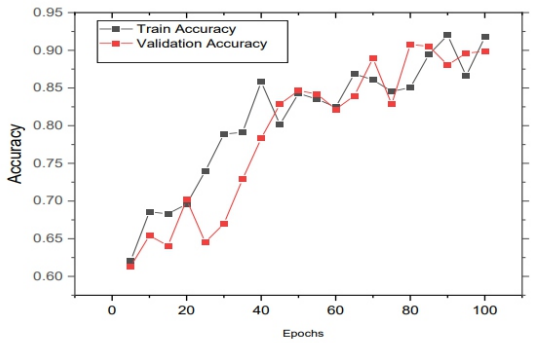

(b)

Figure 5. The Proposed Model Loss (a) and Accuracy (b) Training Graphs in the Customized Cat's Dataset

Furthermore, we used the bar chart to present a comparison of the model's performance across different facial expression categories. It visualizes the distribution of correct and incorrect predictions for each expression category, allowing for a comparative analysis of the model's accuracy and misclassification rates [29]. Figure 6 illustrates the bar chart for achieving the proposed model performance metrics in four domestic cats' expressions. The model achieved excellent results in all four expressions.

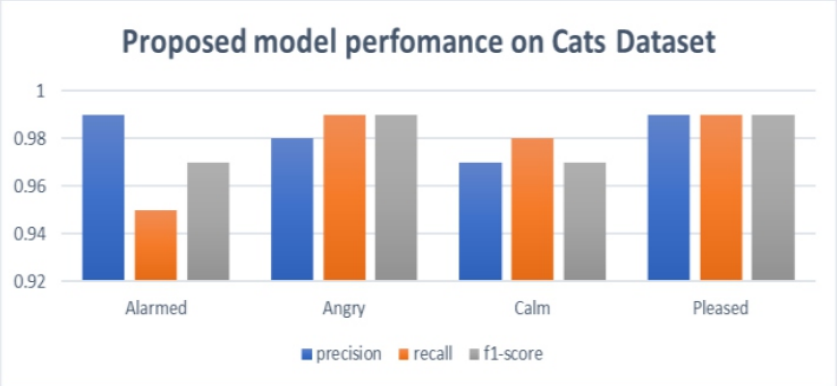

Finally, we assessed the proposed model performance by using a confusion matrix. It displays the distribution of true positive, false positive, true negative, and false negative predictions across different expression categories, offering insights into the model's classification performance [30]. Figure 7 displays the normalized confusion matrix results evaluation of the proposed model on the Customized Cat's dataset.

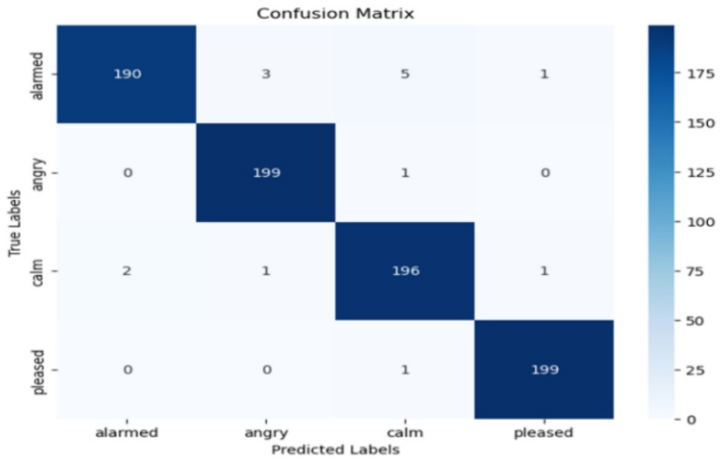

Figure 7. The Heat Map of the Confusion Matrix on the Customized cat's Dataset by the Proposed Model

B.Domestic Cats Facial Expression Recognition Real-time Results by Proposed Model

Real-time Domestic cats' facial expression recognition result is portrayed in Figure 8, the model showcases its agility by accurately identifying and categorizing a spectrum of feline expressions, spanning from 'pleased' and 'happy' to 'alarmed' and 'calm'. This adaptation of the proposed modelhighlights its versatility, extending beyond conventional applications to tackle the complex

domain of feline emotional expression recognition.

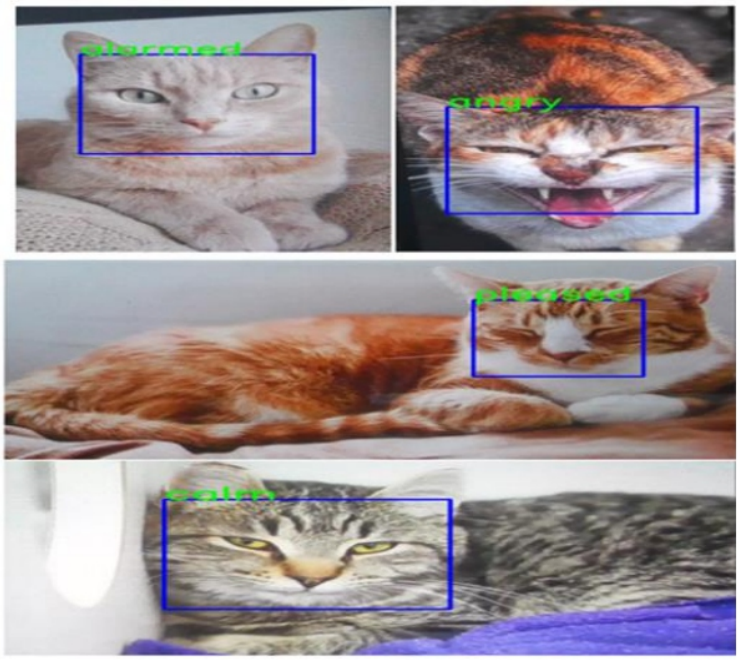

Figure 8. Domestic Cats Real-time Facial Expressions Recognition Results by Proposed model

C.Discussion

The evaluation results of the proposed model on domestic cat's dataset offer valuable insights into the model's performance in classifying emotions within each animal category. The accuracy of the model demonstrates its overall effectiveness in correctly classifying emotions for domesticcats, with accuracies of 98%. While this accuracyy indicate solid performance, it also suggests room for refinement, especially considering the complexities of interpreting animal emotions. Our proposed method may benefit from the introduction of Squeeze-and-Excitation (SE) blocks in our model architecture which enhanced the representational power of a network by enabling it to perform dynamic channel-wise feature recalibration. Table 4. Shows the accuracy results comparison of our customized network with existing studies.

Table 4. The Results Comparison of our Proposed Method with Existing Studies

Method	Optimizer	Accuracy
Proposed Method	Adam	98%
Inception-v3 [31]	Adam	80.42%
Resnet50[32]	Adam	91%

V. CONCLUSION AND FUTURE WORK

A.Conclusion

Our study provides contribution insights into deep learning applications in understanding animal behavior, especially in the context of facial expressions in domestic cats, which is relatively unexplored. These results suggest that the Proposed model is well-suited for the task of recognizing domestic facial expressions, with a particularly strong aptitude for identifying expressions of anger, calmness, and pleasure. Such performance metrics indicate the model's potential applicability in various real-world

scenarios where understanding and interpreting human emotions from facial expressions are crucial, such as in human-computer interaction, emotion recognition systems, and mental health assessment tools. Also, this research contributes to the growing field of animal emotion recognition and opens avenues for developing applications focused on enhancing human-animal interaction and welfare.
However, it's important to note that while these results are promising, further validation and testing in diverse and real-world contexts would be necessary to assess the model's robustness and generalizability. Nonetheless, based on the evaluation report, the Proposed model demonstrates a high level of proficiency in recognizing domestic facial expressions, laying a solid foundation for its potential deployment in practical applications aimed at understanding and responding to human emotions effectively.

B.Future Work

One of the primary areas for future work involves expanding and diversifying the datasets used for training and evaluation. While the current datasets provide valuable insights, they may not fully represent the diversity of emotional expressions and variations within different breeds of cats and dogs. Future work could involve collecting larger and more diverse datasets, encompassing a wider range of breeds, ages, and environmental conditions. Additionally, including more subtle variations in emotional states and expressions would enable the models to generalize better across different scenarios and populations.
Also, by combining different patterns using deep learning algorithms to Investigate the potential benefits of combining Squeeze-and-Excitation (SE) blocks and Exploration of other machine learning techniques or data sources to improve the accuracy and robustness of cat facial expression recognition in a hybrid approach to leverage the strengths.

ACKNOWLEDGMENT

We would like to acknowledge our main supervisor for this project, Prof. Yang Jiachen. He led us to the amazing world of deep learning projects, specifically image processing, guided our research project, and helped us mature. He is the mentor we need, and he provides guidance and advice wherever and whenever we desire. Thank you, Prof. Yang Jiachen, for giving us the opportunity to embark on this great journey we have taken as your students. Also, we would like to thank our fellow laboratory members Xiao Shuai, Lan Guipeng, and Darous K. Joboe for their mentoring during this research project, and last but not least, we would like to acknowledge the School of Electrical Automation and Information Engineering of Tianjin University and College of Software of Nankai University for their continuous support.

DECLARATION STATEMENT

Funding	No, We did not receive any financial support for this article.
Conflicts of Interest	No conflicts of interest to the best of our knowledge.
Ethical Approval and Consent to Participate	No, the article does not require ethical approval and consent to participate with evidence.
Availability of Data and Material	Not relevant.
Authors Contributions	All authors have equal participation in this article.

REFERENCES

1. C. Dalvi, M. Rathod, S. Patil, S. Gite, and K. Kotecha, "A Survey of AI-Based Facial Emotion Recognition: Features, ML & DL Techniques, Age-Wise Datasets and Future Directions," IEEE Access, vol. 9, pp. 165806–165840, 2021, doi: 10.1109/ACCESS.2021.3131733. https://doi.org/10.1109/ACCESS.2021.3131733

2. S. Li and W. Deng, "Deep Facial Expression Recognition: A Survey," IEEE Trans. Affective Comput., vol. 13, no. 3, pp. 1195–1215, Jul. 2022, doi: 10.1109/TAFFC.2020.2981446.https://doi.org/10.1109/TAFFC.2020.2981446

3. L. Dawson, "Are you a cat whisperer? How to read Fluffy's facial expressions," The Conversation. Accessed: Oct. 10, 2023. [Online]. Available: http://theconversation.com/are-you-a-cat-whisperer-how-to-read-fluffys-facial-expressions-128686

4. "Emotions Body Language," Purina.com.au, 2023. https://www.purina.com.au/cats/behaviour/emotions-body-language(accessed Aug. 26, 2023).

5. C. P. Udeh, L. Chen, S. Du, M. Li, and M. Wu, "Multimodal Facial Emotion Recognition Using Improved Convolution Neural Networks Model," Journal of Advanced Computational Intelligence and Intelligent Informatics, vol. 27, no. 4, pp. 710–719, Jul. 2023, doi: 10.20965/jaciii.2023.p0710. https://doi.org/10.20965/jaciii.2023.p0710

6. Azizi, E., & Zaman, L. (2023). Deep learning pet identification using face and body. *Information*, 14(5), 278. https://doi.org/10.3390/info14050278

7. T.-Y. Lin and Y.-F. Kuo, "<i> Cat face recognition using deep learning</i>," in 2018 Detroit, Michigan July 29 - August 1, 2018, American Society of Agricultural and Biological Engineers, 2018.https://doi.org/10.13031/aim.201800316

8. L. Xingxing, "Cat Face Detection Based on Haar Cascade Classifier," in 2019 2nd, CSP, 2019.

9. Y. Fan, C.-C. Yang, and C.-T. Chen, "Cat Face Recognition Based on MFCC and GMM," in 2021 6th International Conference on Image, Vision and Computing (ICIVC), Qingdao, China: IEEE, Jul. 2021, pp. 81–84. https://doi.org/10.1109/ICIVC52351.2021.9527024

10. P. Chen, A. X. Qin, and J. Lu, "Cat Recognition Based on Deep Learning," HAL Archives Ouvertes, Dec. 01, 2021. https://hal.science/hal-03501010/ (accessed Aug. 26, 2023).

11. W. Setiawan, Moh. I. Utoyo, and R. Rulaningtyas, "Classification of neovascularization using convolutional neural network model," TELKOMNIKA (Telecommunication Computing Electronics and Control), vol. 17, no. 1, p. 463, Feb. 2019, doi: https://doi.org/10.12928/telkomnika.v17i1.11604

12. T. N. Tran, B. M. Lam, A. T. Nguyen, and Q. B. Le, "Load forecasting with support vector regression: influence of data normalization on grid search algorithm," International Journal of Electrical and Computer Engineering (IJECE), vol. 12, no. 4, p. 3410, Aug. 2022, doi: https://doi.org/10.11591/ijece.v12i4.pp3410-3420

13. C. P. Udeh, L. Chen, S. Du, M. Li, and M. Wu, "Multimodal Facial Emotion Recognition Using Improved Convolution Neural Networks Model," Journal of Advanced Computational Intelligence and Intelligent Informatics, vol. 27, no. 4, pp. 710–719, Jul. 2023, https://doi.org/10.20965/jaciii.2023.p0710

14. A.-L. Cîrneanu, D. Popescu, and D. Iordache, "New Trends in Emotion Recognition Using Image Analysis by Neural Networks, a Systematic Review," Sensors, vol. 23, no. 16, p. 7092, Aug. 2023, https://doi.org/10.3390/s23167092

15. M. D. Zeiler and R. Fergus, "Visualizing and Understanding Convolutional Networks," Computer Vision – ECCV 2014, pp. 818–833, 2014, https://doi.org/10.1007/978-3-319-10590-1_53

16. A. Krizhevsky, I. Sutskever, and G. E. Hinton, "ImageNet classification with deep convolutional neural networks," Communications of the ACM, vol. 60, no. 6, pp. 84–90, May

2017,https://doi.org/10.1145/3065386
17. S. Lawrence, C. L. Giles, Ah Chung Tsoi, and A. D. Back, "Face recognition: a convolutional neural-network approach," in IEEE Transactions on Neural Networks, vol. 8, no. 1, pp. 98-113, Jan. 1997, https://doi.org/10.1109/72.554195
18. C. Szegedy et al., "Going deeper with convolutions," 2015 IEEE Conference on Computer Vision and Pattern Recognition (CVPR), Boston, MA, USA, 2015, pp. 1-9,https://doi.org/10.1109/CVPR.2015.7298594
19. M. Jogin, Mohana, M. S. Madhulika, G. D. Divya, R. K. Meghana and S. Apoorva, "Feature Extraction using Convolution Neural Networks (CNN) and Deep Learning," 2018 3rd IEEE International Conference on Recent Trends in Electronics, Information & Communication Technology (RTEICT), Bangalore, India, 2018, pp. 2319-2323, https://doi.org/10.1109/RTEICT42901.2018.9012507
20. S. Lawrence, C. L. Giles, Ah Chung Tsoi, and A. D. Back, "Face recognition: a convolutional neural-network approach," in IEEE Transactions on Neural Networks, vol. 8, no. 1, pp. 98-113, Jan. 1997,https://doi.org/10.1109/72.554195
21. S. Shalev-Shwartz and S. Ben-David, Understanding Machine Learning. Cambridge University Press, 2014.https://doi.org/10.1017/CBO9781107298019
22. Hu, Jie, Li Shen, and Gang Sun. "Squeeze-and-excitation networks." In Proceedings of the IEEE conference on computer vision and pattern recognition, pp. 7132-7141. 2018.https://doi.org/10.1109/CVPR.2018.00745
23. K. Thavasimani and N. Kasturirangan Srinath, "Hyperparameter optimization using custom genetic algorithm for classification of benign and malicious traffic on internet of things–23 dataset," International Journal of Electrical and Computer Engineering (IJECE), vol. 12, no. 4, p. 4031, Aug. 2022, https://doi.org/10.11591/ijece.v12i4.pp4031-4041
24. S. Gupta, P. Kumar, and R. K. Tekchandani, "Facial emotion recognition based real-time learner engagement detection system in online learning context using deep learning models," Multimedia Tools and Applications, vol. 82, no. 8, pp. 11365–11394, Sep. 2022, doi: https://doi.org/10.1007/s11042-022-13558-9
25. D. P. Kingma and J. Ba, "Adam: A method for stochastic optimization," in International Conference on Learning Representations (ICLR), 2015.
26. J. Davis and M. Goadrich, "The relationship between Precision-Recall and ROC curves," in Proceedings of the 23rd international conference on Machine learning, 2006, pp. 233-240.https://doi.org/10.1145/1143844.1143874
27. S. Ravidas and M. A. Ansari, "Deep learning for pose-invariant face detection in unconstrained environment," International Journal of Electrical and Computer Engineering (IJECE), vol. 9, no. 1, p. 577, Feb. 2019, https://doi.org/10.11591/ijece.v9i1.pp577-584
28. M. Sokolova, N. Japkowicz, and S. Szpakowicz, "Beyond accuracy, F-score and ROC: a family of discriminant measures for performance evaluation," in Proceedings of the Twenty-Second International Conference on Machine Learning, 2005, pp. 947-954.https://doi.org/10.1007/11941439_114
29. L. Rasheed, U. Khadam, S. Majeed, S. Ramzan, M. S. Bashir, and M. M. Iqbal, "Face Recognition Emotions Detection Using Haar Cascade Classifier and Convolutional Neural Network," In Review, preprint, Nov. 2022. https://doi.org/10.21203/rs.3.rs-2048290/v1
30. R. B. Kala, N. S. Gill, and A. K. Verma, "A comparative analysis of classification algorithms using confusion matrix for intrusion detection system," in 2016 2nd International Conference on Applied and Theoretical Computing and Communication Technology (iCATccT), 2016, pp. 547-552.
31. R. Zhang, "Classification and Identification of Domestic Cats based on Deep Learning," in 2021 2nd

International Conference on Artificial Intelligence and Computer Engineering (ICAICE), pp. 106-110, IEEE, 2021. https://doi.org/10.1109/ICAICE54393.2021.00029

32. Wu, Yujie. "Emotion Detection of Dogs and Cats Using Classification Models and Object Detection Model." 2023.

33. Kumari, J., Patidar, K., Saxena, Mr. G., & Kushwaha, Mr. R. (2021). A Hybrid Enhanced Real-Time Face Recognition Model using Machine Learning Method with Dimension Reduction. In Indian Journal of Artificial Intelligence and Neural Networking (Vol. 1, Issue 3, pp. 12–16). https://doi.org/10.54105/ijainn.b1027.061321

34. P A, J., & N, A. (2022). Faceium–Face Tracking. In Indian Journal of Data Communication and Networking (Vol. 2, Issue 5, pp. 1–4). https://doi.org/10.54105/ijdcn.b3923.082522

35. Maddileti, T., Rao, G. S., Madhav, V. S., & Sharan, G. (2019). Home Security using Face Recognition Technology. In International Journal of Engineering and Advanced Technology (Vol. 9, Issue 2, pp. 678–682). https://doi.org/10.35940/ijeat.b3917.129219

AUTHORS PROFILE

Abubakar Ali, Received B.Eng. degree in Electronics and Communication Engineering from St. Joseph University in Tanzania, Dar es Salaam Tanzania in 2014. He is currently pursuing an M.S. degree in Information and Communication Engineering at the School of Electrical Automation and Information Engineering, Tianjin University, Tianjin, China.
His research interests include image processing and pattern recognition, Computer Vision, Deep learning, and wireless communications.

Crista Lucia Nchama Onana Oyana, Received a B.S. in Measurement Technology and Control Instrumentation from Hebei University of Technology, Tianjin, China in 2020. She is currently pursuing an M.S. degree at the School of Electrical Automation and Information Engineering, Tianjin University, Tianjin, China. Her research interest includes facial emotion detection, computer vision and pattern recognition, and wireless communications.

Othman Saleh Salum, Received a B.S. in Information Technology from the Institute of Finance Management (IFM), Dar es Salaam Tanzania in 2012. He is currently pursuing a M.S. degree in Software Engineering at Nankai University, Tianjin, China. His research interests include face analysis, computer vision, and image processing & pattern recognition.

Instructions for Authors

Essentials for Publishing in this Journal

1 Submitted articles should not have been previously published or be currently under consideration for publication elsewhere.

2 Conference papers may only be submitted if the paper has been completely re-written (taken to mean more than 50%) and the author has cleared any necessary permission with the copyright owner if it has been previously copyrighted.

3 All our articles are refereed through a double-blind process.

4 All authors must declare they have read and agreed to the content of the submitted article and must sign a declaration correspond to the originality of the article.

Submission Process

All articles for this journal must be submitted using our online submissions system. http://enrichedpub.com/ . Please use the Submit Your Article link in the Author Service area.

Manuscript Guidelines

The instructions to authors about the article preparation for publication in the Manuscripts are submitted online, through the e-Ur (Electronic editing) system, developed by **Enriched Publications Pvt. Ltd**. The article should contain the abstract with keywords, introduction, body, conclusion, references and the summary in English language (without heading and subheading enumeration). The article length should not exceed 16 pages of A4 paper format.

Title

The title should be informative. It is in both Journal's and author's best interest to use terms suitable. For indexing and word search. If there are no such terms in the title, the author is strongly advised to add a subtitle. The title should be given in English as well. The titles precede the abstract and the summary in an appropriate language.

Letterhead Title

The letterhead title is given at a top of each page for easier identification of article copies in an Electronic form in particular. It contains the author's surname and first name initial .article title, journal title and collation (year, volume, and issue, first and last page). The journal and article titles can be given in a shortened form.

Author's Name

Full name(s) of author(s) should be used. It is advisable to give the middle initial. Names are given in their original form.

Contact Details

The postal address or the e-mail address of the author (usually of the first one if there are more Authors) is given in the footnote at the bottom of the first page.

Type of Articles

Classification of articles is a duty of the editorial staff and is of special importance. Referees and the members of the editorial staff, or section editors, can propose a category, but the editor-in-chief has the sole responsibility for their classification. Journal articles are classified as follows:

Scientific articles:

1. Original scientific paper (giving the previously unpublished results of the author's own research based on management methods).

2. Survey paper (giving an original, detailed and critical view of a research problem or an area to which the author has made a contribution visible through his self-citation);

3. Short or preliminary communication (original management paper of full format but of a smaller extent or of a preliminary character);

4. Scientific critique or forum (discussion on a particular scientific topic, based exclusively on management argumentation) and commentaries. Exceptionally, in particular areas, a scientific paper in the Journal can be in a form of a monograph or a critical edition of scientific data (historical, archival, lexicographic, bibliographic, data survey, etc.) which were unknown or hardly accessible for scientific research.

Professional articles:

1. Professional paper (contribution offering experience useful for improvement of professional practice but not necessarily based on scientific methods);
2. Informative contribution (editorial, commentary, etc.);
3. Review (of a book, software, case study, scientific event, etc.)

Language

The article should be in English. The grammar and style of the article should be of good quality. The systematized text should be without abbreviations (except standard ones). All measurements must be in SI units. The sequence of formulae is denoted in Arabic numerals in parentheses on the right-hand side.

Abstract and Summary

An abstract is a concise informative presentation of the article content for fast and accurate Evaluation of its relevance. It is both in the Editorial Office's and the author's best interest for an abstract to contain terms often used for indexing and article search. The abstract describes the purpose of the study and the methods, outlines the findings and state the conclusions. A 100- to 250-Word abstract should be placed between the title and the keywords with the body text to follow. Besides an abstract are advised to have a summary in English, at the end of the article, after the Reference list. The summary should be structured and long up to 1/10 of the article length (it is more extensive than the abstract).

Keywords

Keywords are terms or phrases showing adequately the article content for indexing and search purposes. They should be allocated heaving in mind widely accepted international sources (index, dictionary or thesaurus), such as the Web of Science keyword list for science in general. The higher their usage frequency is the better. Up to 10 keywords immediately follow the abstract and the summary, in respective languages.

Acknowledgements

The name and the number of the project or programmed within which the article was realized is given in a separate note at the bottom of the first page together with the name of the institution which financially supported the project or programmed.

Tables and Illustrations

All the captions should be in the original language as well as in English, together with the texts in illustrations if possible. Tables are typed in the same style as the text and are denoted by numerals at the top. Photographs and drawings, placed appropriately in the text, should be clear, precise and suitable for reproduction. Drawings should be created in Word or Corel.

Citation in the Text

Citation in the text must be uniform. When citing references in the text, use the reference number set in square brackets from the Reference list at the end of the article.

Footnotes

Footnotes are given at the bottom of the page with the text they refer to. They can contain less relevant details, additional explanations or used sources (e.g. scientific material, manuals). They cannot replace the cited literature.
The article should be accompanied with a cover letter with the information about the author(s): surname, middle initial, first name, and citizen personal number, rank, title, e-mail address, and affiliation address, home address including municipality, phone number in the office and at home (or a mobile phone number). The cover letter should state the type of the article and tell which illustrations are original and which are not.